Utrecht University

UMC Utrecht

Uncovering the mechanism of action of cardiac arrhythmias caused by cancer therapeutics that target the hERG channel: A Literature review

Author: Roxy Finger (3587969)

Degree: Drug Innovation (MSc)

Daily supervisor: M. Bloothooft

Examinator: Dr. M.A.G. van der Heyden

Date: 15-07-2022

Abstract

Over the years, tremendous progression in development of cancer treatments has taken place with more cancer survivors as a result. As more cancer-survivors live with the long-term effects of the cancer treatments and will eventually deal with age-related diseases such as cardiovascular diseases, the cardiovascular risk factors are magnified, and complications may lead to morbidity and mortality in cancer survivors. Anticancer drugs can lead to drug-induced arrhythmias by either direct or indirect changes, where the former could lead to the inhibition of the rapid component of the delayed rectifier K^+ channel (I_{Kr}) which prolongs the QTc interval and eventually to the life-threatening ventricular arrhythmia Torsades de Pointes (TdP). The inhibition of I_{Kr} is related to the blockage of the human ether-à-go-go related gene (hERG) potassium channel as this channel plays a role in the repolarization of the heart ventricles. Gaining more knowledge about the binding mechanisms of the different chemotherapeutic drugs that target this channel may help the development of new chemotherapeutic agents without the adverse cardiotoxicity.

In this review, the mechanism by which the hERG channel is inhibited by several chemotherapeutic drugs was assessed. The two mechanisms to inhibit the hERG channel are by either binding to the F656 and/or Y652 aromatic residues in the binding pocket of hERG, creating a direct blockage of the channel, or inhibiting the trafficking of the fully glycosylated hERG channels to the cell surface by inhibiting the hERG-Hsp90 complex formation. Further research should be performed to elucidate the exact molecules that bind to the residues in the binding pocket and Hsp90 inhibition, which may lead to hERG channel degradation, should be accounted for when developing new chemotherapeutic agents. Agents that target the hERG channel, but do not induce arrhythmias, should still be carefully monitored in older patients as they have an increased risk of proarrhythmogenic events. Elucidating the mechanism of the inhibition will make the development of new chemotherapeutic agents safer, even for the aging population.

Layman's summary

Cancer is the second leading cause of death worldwide behind cardiovascular disease. This is because cancer is caused by the abnormal growth of any cell type in the body, so there are more than a hundred different kinds of cancer. In the past years, the development of anticancer drugs has reduced the number of deaths. However, age-related diseases, such as cardiovascular diseases (CVD), become a greater problem as cancer survivors get older. The complications of the development of these CVDs may lead to more morbidity and death in the cancer survivors. Anticancer drugs can produce heart rhythm disorders by inhibiting ion channels in the heart and these disorders can even lead to the life-threatening heart rhythm disorder Torsades de Pointes (TdP). Heart rhythm disorders is one of the most frequent adverse effects, leading to the discontinuation of drugs. This discontinuation is mostly related to the ability of the drugs to inhibit the human ether-à-go-go related gene (hERG) ion channel and this channel plays a vital role in the cardiac action potential. Potassium ions pass through the hERG channel during repolarization of the heart. Inhibiting this channel will cause a longer repolarization period which can lead to heart rhythm disorders.

The ion channel consists of six segments, which are lined up next to each other on the cell membrane. The four inner segments form the channel, where the K^+ ions pass through the channel, but this is also one of the places where compounds can bind to the hERG channel. Bound compounds are in the channel pore and block the passing of the ions. An immature form of the hERG channel is first synthesized in the endoplasmic reticulum after it is transferred to the Golgi apparatus. In the Golgi apparatus, the immature form is fully glycosylated and transported to the plasma membrane. The anticancer drugs that inhibit the hERG channel most often block the hERG channel by binding to the channel or prevent the fully glycosylated channel to be transported to the plasma membrane. However, how anticancer drugs exactly block or inhibit the transportation of the hERG channel is often not known. In this review, the different groups of anticancer drugs have been studied to find out if they inhibit the hERG channel and how they inhibit the channel.

There has been found that most anticancer drugs block the hERG channel by binding to two specific amino acids in the channel, which contain an aromatic ring, or they inhibit the heat shock protein 90 (Hsp90). This protein has been found to help the transportation of the immature channel from the endoplasmic reticulum to the Golgi system. The anticancer drugs bind to Hsp90, so it cannot help the transportation of the hERG channel, and the immature channel cannot be glycosylated to the mature channel. Furthermore, some anticancer drugs do inhibit the hERG channel but that does not lead to heart rhythm disorders in healthy, young people. If these drugs are given together or to older people, this could lead to heart rhythm disorders, even though they did not cause disorders in the clinical trials. Therefore, all anticancer drugs should be monitored carefully when given to patients for causing heart rhythm disorders and studying how the anticancer drugs bind to the amino acids in the channel and how they inhibit Hsp90 will give more information to design new anticancer drugs that do not inhibit the hERG channel and cannot cause heart rhythm disorders.

Table of contents

1. Introduction

The early detection of cancer and the cancer treatments that were developed in recent years have reduced the mortality and morbidity of cancer patients tremendously[1,2]. However, as cancer is an age-related disease and the life-expectancy has risen, the occurrence of cardiovascular risk factors is magnified, and complications may lead to morbidity and death in cancer survivors[2–4]. Therefore, cardiovascular disease (CVD) is a major complication of cancer treatments[5,6]. Drug induced arrhythmias can lead to direct and indirect changes. Indirect changes of drug induced arrhythmias, such as remodeling of the heart and inflammation, can create a structural arrhythmia substrate. Direct changes of drug induced arrhythmias can lead to the modification of specific molecular pathways, which could inhibit the rapid component of the delayed rectifier K^+ channel (I_{Kr}), thereby prolonging the corrected QT (QTc) interval[3]. Prolongation of the QTc might even lead to life-threatening ventricular arrhythmia Torsades de Pointes (TdP)[7].

The hERG channel plays a role in the action potential (AP) of cardiac ventricular myocytes as the I_{Kr} current together with the slow delayed rectifier current (I_{Ks}) play a vital role in the repolarization of the heart ventricles[8]. The inhibition of I_{kr} is most often related to the blockage of the human ether-à-go-go related gene (hERG) potassium channel[9]. The human ether-à-go-go related gene (officially called *KCNH2*) encodes the pore-forming α-subunit of the rapid component of the delayed rectifier K^+ channel (I_{Kr})[8]. The hERG channels (also known as Kv11.1[10]) belong to the Eag (ether-à-go-go) family, which is a multi-genic family of voltage-activated K^+ channels[11]. Research has shown that mutations in *KCNH2* caused the chromosome 7-associated long QT syndrome (LQTS type 2)[12] and that the hERG channels were the targets of class III antiarrhythmic drugs[13].

However, a lot of different non-antiarrhythmic drugs (such as antibacterials, antihistamines, antipsychotics and anti-human immunodeficiency protease inhibitors[14]) have also shown to be pro-arrhythmic and most of them are I_{kr} blockers blocking the hERG channel[15]. Therefore, during the pre-clinical studies of new compounds, the QT liability (the potential to prolong the QT interval) is assessed[11]. It is estimated that as high as 60% of the new potential drug compounds block the hERG channel and are thus abandoned in the development stage[16]. Gaining more knowledge about the drug structures that target the hERG channel and the mechanism of actions how the channel is targeted may reduce the number of abandoned potential drug compounds.

The mRNA of hERG undergoes post-transcriptional modifications (PTMs) resulting in four isoform variations and these variants have different electrophysiological properties[17]. In this review, the focus will be on the largest hERG isoform (isoform a). The hERG channel consists of six transmembrane segments (S1-S6) forming a homotetramer[18], S1-S4 are part of the voltage sensor domain (VSD) and S5-S6, together with the intervening loop, are part of the pore domain[8] (**Figure 1**). The movements of the VSD enables opening and closing of the channel in response to membrane potential changes[19]. The pore domain contains the pore helix and selectivity filter for the passage of K^+ ions[19]. The drug binding site is a tetramer and the pore domains of the four subunits line the central ion conduction pathway. The residues Thr623, Ser624 and Val625 have been shown to be involved in drug binding and are located at the base of the selectivity filter[20–22]. The residues Gly648, Tyr652, Phe656 and Val659 have been shown to be involved in drug binding and are located on the same face of S6. The hERG channel also contains a large cytoplasmic NH_2-terminal containing a Per-Arnt-Sim (PAS) domain[23] and COOH-terminal domains containing a cyclic nucleotide binding domain (cNBD)[24].

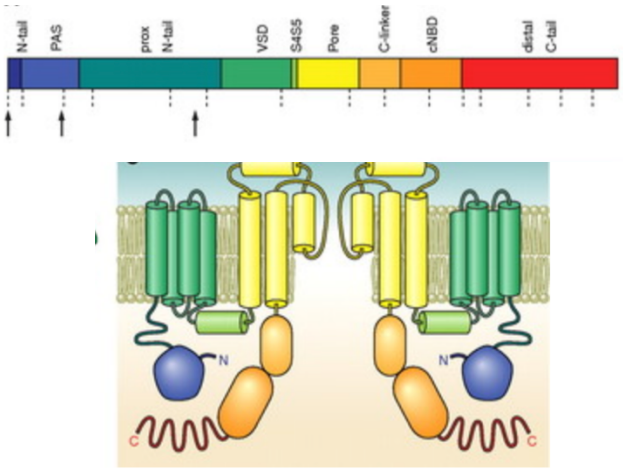

Figure 1. Structure of the hERG channel with a linear sequence with the domains color coded[8].

The immature hERG protein is modified post-translation through glycosylation and phosphorylation to become the mature form of hERG[18]. The immature form has a core-glycosylated monomer and is synthesized in the endoplasmic reticulum after which it is transferred to the Golgi apparatus. In the Golgi apparatus, the immature form is fully glycosylated, and this mature form is transported to the plasma membrane in COPII coated vesicles where the channels are used for K^+ conductance[25]. This shows that glycosylation is critical for trafficking efficiency and it prevents the cleavage of the channel by extracellular proteinase K (PK)[26,27].

The channel can exist in a closed, open or inactivated state depending on the voltage[8]. The positive charges in the S4 domain acts as the primary sensor for channel opening[28]. The hERG channel is closed at negative membrane potentials, but when the AP starts with activation of the inward Na^+ current, the depolarization of the cell membrane results in the short opening of the hERG channel[8,18,29]. After opening, the channel transitions fast to the inactivated state reducing the outward conductance. After depolarization, gradual repolarization takes place in three subsequent phases. First, rapid repolarization occurs, which is created by the activation of the transient outward K^+ current (I_{to}) after which a plateau phase takes place[29]. This reduces the membrane potential causing the hERG channels to change from the inactivated state to open state. This results in a big outward conductance of K^+ and thus the repolarization of the cell. The transition from open to closed state is very slowly, so the hERG channel remains open after the membrane potential has returned to resting level causing hyperpolarization[8]. If there is a premature beat, the large increase in I_{Kr} antagonizes the depolarization of a cell and this large increase is due to the slow closing of the hERG channels[30]. This shows the role of hERG by the suppression of arrhythmias initiated by premature beats. When the I_{Kr} is reduced by loss-of-function mutations or drug block, the patient will be more prone to arrhythmias.

The anticancer drugs that target hERG most often block the hERG channel or prevent the trafficking of the channel to the plasma membrane, but the exact underlying mechanism is still unknown[15]. Therefore, the different groups of anti-cancer drugs will be reviewed that target the hERG channel and their structure and mechanism of action targeting the channel will be highlighted. Furthermore, different drugs from the same group of pharmaceuticals show differences in the QTc prolongation so this article will elucidate the cause of these differences. The findings in this review can be used to develop new potential cancer treatments that do not target the hERG channel and do not induce arrhythmias.

2. Anticancer Drug-Induced Proarrhythmia

2.1 Arsenic Trioxide

Arsenic Trioxide (ATO) is a drug for treating acute promyelocytic leukemia (APL). 20-30% of patients with APL relapse with the standard chemotherapy regimen and studies showed that up to 90% of patients with APL achieved complete remission after treatment with ATO[31]. However, > 10% of the patients receiving ATO have been associated with tachycardia and QT prolongation[32]. In clinical trials, 40% of the patients experienced one or more QTc interval prolongations greater than 500 msec[33]. As most patients were first treated with cardiotoxic chemotherapy before receiving ATO, most of them have cardiac dysfunction before the start of ATO treatment[31]. A study by *Chiang et. al*.[34] showed that ATO dose dependently prolonged corrected QT interval (QTc) and the action potential duration at 90% repolarization (ADP90) in guinea pig hearts providing evidence for ATO delaying cardiac repolarization.

Structure

ATO is a small arsenic compound with the chemical formula As_2O_3 and used to inhibit and spread the growth of tumors (also known as antineoplastic drugs) (**Figure 2**)[35,36].

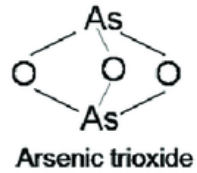

Figure 2. Chemical structure of Arsenic Trioxide by *Khairul et al*.[36]

Mechanism of action

The mechanism underlying the prolonged QTc and ADP90 was shown by *Ficker et. al.*[37], who discovered that long-term exposure to ATO increases cardiac calcium currents via oxidative interaction of the lipid phosphatase PTEN[38] and reduces surface expression of hERG by inhibiting the formation of the channel-chaperone (Hsp70/90) complexes[37]. The cytosolic chaperones heat shock protein (Hsp) Hsp70 and Hsp90 interacted with the core-glycosylated form of hERG in the ER but did not interact with the fully glycosylated, cell-surface form of hERG. This indicates that Hsp90 and 70 are both crucial for the maturation of hERG[39]. ATO interferes with binding of Hsp90 and 70 to the core-glycosylated form of hERG by interacting with the thiol pair in the middle segment of the chaperone protein Hsp90[40]. Modification of these thiol groups might inhibit the binding of Hsp90 to the core-glycosylated form of hERG and thus inhibits the processing of the ER-resident hERG protein into the mature cell-surface form[37]. Therefore, long-term exposure to ATO reduces surface expression of the hERG channel, resulting in a reduction of $I_{Kr.}$ This reduction prolongs the QT interval, which could lead to TdP in patients treated with ATO.

Clinical relevance

Ficker et. al.[37] showed that neither 10 nor 100 µM ATO applied extracellularly reduced hERG tail current amplitudes within 10 to 15 min. In contrast, they found a reduction in hERG current in a concentration-dependent manner with an IC_{50} of 1.5 µM after 24 hours of exposure to ATO (**Figure 3A**). They found this IC_{50} by analyzing tail current amplitudes on return to -50 mV after maximal activation with depolarizing voltage steps to +60 mV in HEK293 cells stably expressing hERG. During ATO treatment in APL patients, the ATO concentrations peak between 5 and 10 µM immediately after drug administration and reach steady-state levels between 0.1 and 1 µM, which shows that the found IC_{50} of 1.5 µM is within therapeutically relevant concentration range of ATO[41]. Furthermore, their Western blot analysis showed a time- and concentration-dependent decrease in amount of mature, fully glycosylated hERG protein after incubation with ATO for 24 hours (**Figure 3B**). The production of the fully glycosylated hERG form was suppressed with an IC_{50} of 1.5 µM, which was in line with the

reduced currents. On top of this, their chemiluminescence assay performed in HEK293 cells stably expressing hERG with an extracellular HA epitope tag inserted in the extracellular S1 to S2 loop showed a significant concentration-dependent reduction in hERG surface expression after overnight treatment with ATO (**Figure 3C**). Next, their pulse-chase experiments performed on myocytes as a control, showed that after treatment with 3 µM ATO, 50% of the core-glycosylated hERG form was progressed to the mature cell-surface hERG form within 6 hours. Treating HEK-hERG cells with 3 µM ATO for 16 hours before the pulse-chase experiment, showed a 25% reduction of maturation. Lastly, their coimmunoprecipitation experiments in a HEK/hERG WT cell line showed an approximately 50% inhibition of the formation of the hERG/Hsp90 complexes when treated with 3 µM ATO overnight and an approximately 20% inhibition of the formation of the hERG/Hsp70 complexes (**Figure 3D**). This shows that ATO predominantly blocks the formation of the hERG/Hsp90 complexes, which inhibits the trafficking of the immature hERG form to the Golgi system resulting in less fully mature cell-surface channels[37].

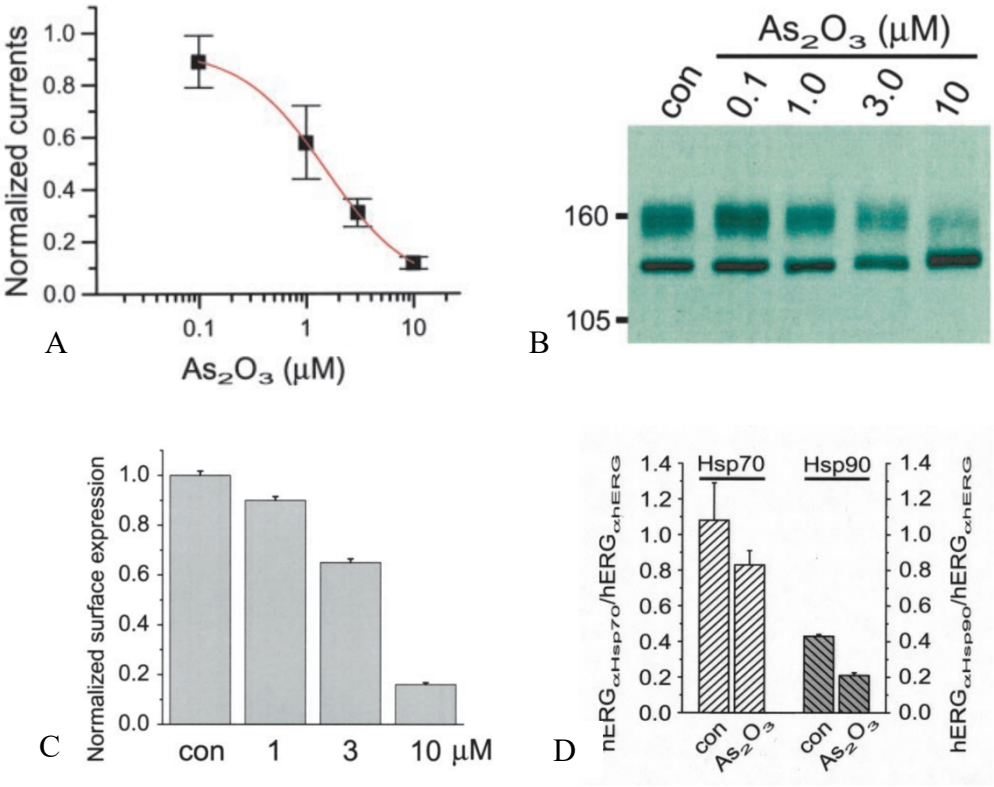

Figure 3. Graphs by *Ficker et. al.*[37] showing the effect of ATO on HEK293 cells stably expressing hERG.
A) ATO showed a concentration-dependent reduction of hERG tail current amplitudes after overnight exposure of ATO with an IC_{50} of 1.5 µM.
B) Western blot showed a time- and concentration-dependent decrease in amount of mature, fully glycosylated hERG protein (155 kDa) after incubation with ATO for 24 hours on hERG WT protein stably expressed in HEK293 cells.
C) The chemiluminescence assay performed in HEK293 cells stably expressing hERG with an extracellular HA epitope tag inserted in the extracellular S1 to S2 loop showed a significant concentration-dependent reduction in hERG surface expression after overnight treatment with ATO.
D) The coimmunoprecipitation experiments in a HEK/hERG WT cell line showed an approximately 50% inhibition of the formation of the hERG/Hsp90 complexes when treated with 3 µM ATO overnight and an approximately 20% inhibition of the formation of the hERG/Hsp70 complexes.

2.2 Topoisomerase inhibiters

Amsacrine

Amsacrine (m-AMSA) is a topoisomerase II inhibitor and used for treating refractory acute leukemias, Hodgekin's and non-Hodgekin's lymphomas[42]. M-AMSA kills cells by intercalating into DNA and inhibiting the DNA topoisomerase II. In acute myelogenous leukemia, m-AMSA can produce complete remission in patients[43]. However, m-AMSA treatment has been associated with QT interval prolongation, ventricular arrythmia and death[44–46]. 1 – 10% of the patients treated with m-AMSA have experienced cardiac arrhythmias and hypokalaemia[47]. Patients with hypokalaemia have an increased risk of ventricular fibrillation[33]. 0.01 – 0.1% of the patients treated with m-AMSA have experienced cardiomyopathy, atrium and/or ventricular fibrillation, sinus tachycardia or bradycardia[46]. This might indicate that m-AMSA has an effect on cardiac repolarization and may affect the hERG channel. M-AMSA is frequently used with other antineoplastic agents who could inhibit the hERG channel as well. Therefore, the effect of m-AMSA on cardiac repolarization should be elucidated as adverse effects of m-AMSA may be potentiated by use with other antineoplastic agents[48].

Structure

Amsacrine is an acridine derivate with the chemical name $C_{21}H_{19}N_3O_3S$. It is a N-phenylmethanesulfonamide substituted by a methoxy group at the third position and an acridin9-ylamino group at the fourth position (**Figure 4**)[43,49].

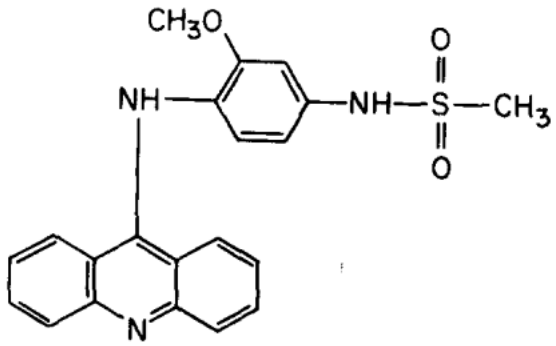

Figure 4. Chemical structure of Amsacrine by *Cassileth et al.*[49]

Mechanism of action

Amsacrine inhibits hERG channels predominantly in the open and inactivated state. M-AMSA binds to the aromatic residues of F656 and partly to Y652 within the pore-S6 region[48]. After binding to the aromatic residues, it is most likely that m-AMSA is trapped at its binding site when the hERG channel inactivates and m-AMSA gets released again after the opening of the channel. This prolongs the blocking effect and as the unblocking of m-AMSA was slow, this trapping mechanism could be the cause[50,51]. Blocking of m-AMSA was found to be voltage-independent[48]. Relative inhibition of peak currents was not significantly different among the voltage steps (-40, 0, 40 and 80 mV) after superfusion of 3 µM m-AMSA for 15 min in oocytes. Furthermore, no significant changes in the amount of steady-state block at both rates (1 and 0.1 Hz) were measured in the presence of 3 µM m-AMSA on oocytes[48]. Therefore, the m-AMSA block was also not frequency dependent.

Clinical relevance

Thomas et. al.[48] showed that the hERG channels were blocked in a concentration-dependent manner in *Xenopus laevis* oocytes. The half-maximal inhibition concentration (IC_{50}) was 2.0±0.1 μM (**Figure 5A**). After a control period of 20 minutes, the hERG block by 10 μM m-AMSA reached steady-state conditions after 10 to 15 minutes. Upon 20 min of washout, the blocking effects were partially reversible. This concentration-dependent block was also seen in HEK293 cells stably transfected with hERG, with a IC_{50} of 209.4±6.0 nM (**Figure 5B**). The 9.6-fold difference in IC_{50} values for the two systems are due to the properties of the Xenopus laevis oocytes expression system. As this system also consists of a vitelline membrane and the yolk, it reduces the actual concentration of drugs at the cell membrane. Therefore, higher concentrations of drugs are necessary when applied to whole oocytes under in vitro conditions. Furthermore, the effect of m-AMSA on hERG current voltage (I-V) relationship was studied under isochronal recording conditions after exposure to 3 μM m-AMSA for 15 minutes in the oocytes. The currents of hERG at the end of the test pulse to 0 mV were reduced by 38.8±3.0% (**Figure 5C and D**) and peak tail currents were blocked by 44.3±1.7%. The half-maximal activation voltage $V_{1/2}$ was shifted by -7.6±0.8 mV. No changes in time constants of inactivation were observed after 3 μM m-AMSA block for 15 min in oocytes. In contrast, the steady-state inactivation relationships were measured in the oocytes after exposure to 3 μM m-AMSA for 15 min and they showed that the half-maximal inactivation voltage displayed a relative shift of -7.6±0.8 mV. They suggest that this shift could be interpreted as drug-induced effect on hERG inactivation. The therapeutic m-AMSA plasma concentrations in humans have been reported to be 5-18 μM[52,53] and the study by *Thomas et. al.*[48] showed the effects of m-AMSA with 3 and 10 μM m-AMSA indicating that the block of m-AMSA is at clinically relevant concentrations.

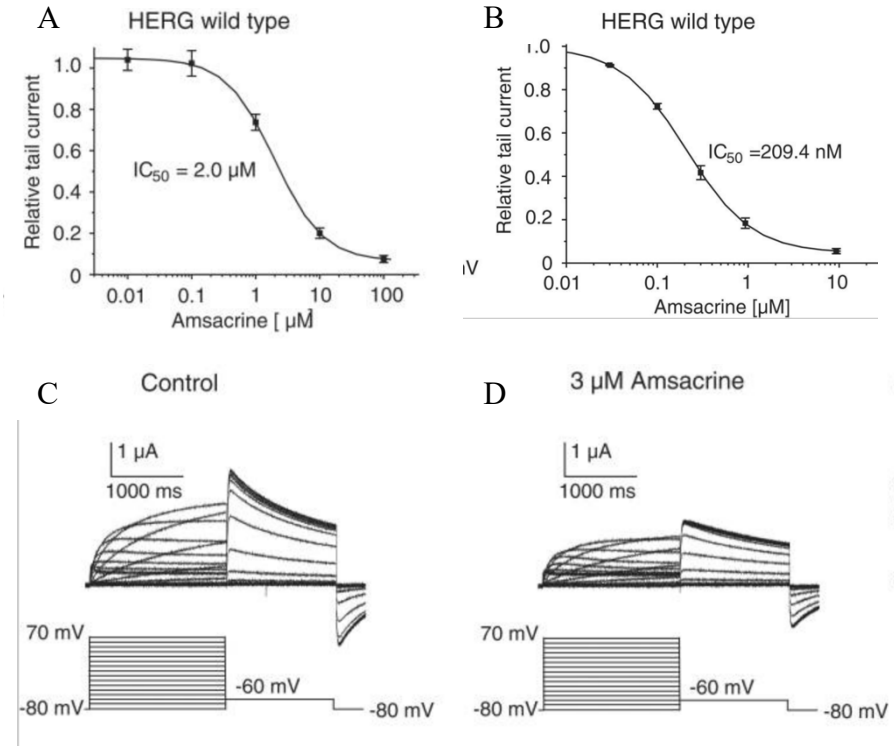

Figure 5. Graphs by *Thomas et. al.*[48] showing the effect of m-AMSA on *Xenopus laevis* oocytes and HEK293 cells stably transfected with hERG.

A) hERG channels were blocked in a concentration-dependent manner in oocytes with an IC_{50} of 2.0 µM.

B) A concentration-dependent block in HEK293 cells stably transfected with hERG, with a IC50 of 209.4 nM.

C) hERG currents as control measurements.

D) 3 µM m-AMSA present for 15 min in one representative oocyte, reduced the hERG currents by 38.8%.

2.3 Hsp90 inhibitors

Geldanamycin and 17-AAG

Geldanamycin (GA) is a heat shock protein 90 (Hsp90) inhibitor and as Hsp90 is required for the stability and function of proteins that promote growth and/or survival of cancer cells, geldanamycin and other Hsp90 inhibitors were of interest to function as cancer treatments[54]. Geldanamycin is cytotoxic to several human cancer cell lines, including breast cancer, thyroid cancer and bladder cancer[55–57]. 1 -10% of patients treated with AG experienced brady- or tachycardia[32]. 0.1 – 1% of the patients treated with A experienced cardiomyopathy, asymptomatic ventricular tachycardia, AV-block or myocardial infraction. GA has been shown to be too hepatoxic for clinical use, but the derivate 17-allylamino-17-demethoxygeldanamycin (17-AAG or Tanespimycin) also bound to Hsp90, was less toxic and showed promising antitumor activity[54,58]. However, Hsp90 and also Hsp70 might interact with newly synthesized hERG channels, so inhibition of Hsp90 or Hsp70 by GA or 17-AAG might also inhibit the maturation of the hERG channels leading to arrhythmias and GA has already be linked to an increased risk for QTc interval prolongation and associated arrhythmias[59,60,61].

Structure

GA is a benzoquinone antibiotic isolated from the bacterium Streptomyces hygroscopicus. The chemical name of GA is $C_{29}H_{40}N_2O_9$ and it is an ansamycin, an organic heterobicyclic compound, a carbamate ester and a member of the 1,4-benzoquinones (**Figure 6A**)[62]. The ansamycin has 19-membered macrocycle including a benzoquinone ring and a lactam functionality[63]. 17-AAG is also a benzoquinone antibiotic derived from GA and in this 19-membered macrocyle is the methoxy substituent attached to the benzoquinone moiety replaced with an allylamino group[64]. The chemical name of 17-AAG is $C_{31}H_{43}N_3O_8$ (**Figure 6B**)[65].

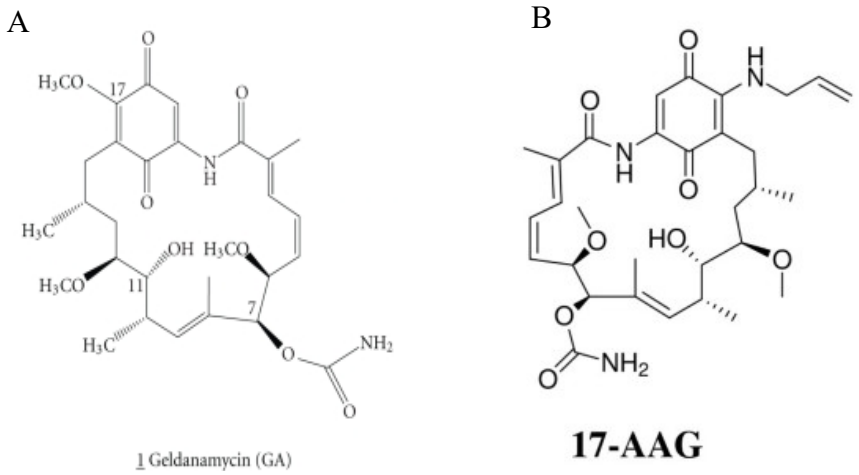

Figure 6. Chemical structures of **A**) geldanamycin by *Wenkert et. al*.[62] and **B**) its derivate 17-AAG by *Mout et. al*.[65]

Mechanism of action

The binding site of Hsp90 is a pocket of 15 Å deep and GA binds inside this pocket adopting a compact structure[66]. GA has its macrocyclic ansa ring and pendant carbamate group directed towards the bottom of the binding pocket and the benzoquine ring is directed towards the top of the pocket as it opens to the surface of the domain[67]. This domain also binds ATP linked to Sepharose through the γ-phosphate and this binding is specific for ATP and ADP and ATP is essential for the formation of an Hsp90 state that is stable to bind one of its partner proteins p23[68]. The binding of GA thus inhibits the ATPase cycle of Hsp90 leading to interruption of the Hsp90-mediated conformational maturation/refolding reaction and therefore Hsp90 substrates are degraded[66]. This leads to less Hsp90 complexes, which controls the folding and maturation of the hERG channel. On top of this, GA prevents the formation of the Hsp90-hERG complexes by blocking the functionally important ATPase activity of Hsp90. This prevents the maturation of the hERG channels into the fully glycosylated cell surface form. This indicates that GA

inhibits hERG in two ways, it increases proteasomal degradation of hERG channels and it inhibits the formation of Hsp90-hERG complexes preventing the maturation of the channels.

Clinical relevance

A study by *Ficker et. al.*[59] showed a time-dependent decrease in mature, fully glycosylated hERG protein after incubation with GA. The hERG currents were also reduced after HEK293 cells stably transfected with hERG WT were cultured overnight in the presence of 1 µg/mL GA (**Figure 7A**). Acute application of GA had no effect on the hERG currents. Furthermore, treatment with 1 and 10 µmol/L GA showed a reduced expression of fully glycosylated hERG protein. They also showed a significant reduction in tail current amplitudes from 187.8±21.2 to 92.1±12.7 pA/pF and 82.2±14.0 pA/pF with 1 µmol/L and 10 µmol/L GA treatment, respectively. On top of this, pulse-chase experiments showed that in control cells, about 50% of the core-glycosylated protein was converted into the mature fully glycosylated protein within 4 hours, while only small amounts of fully glycosylated protein were produced in HEK293 cells stably transfected with hERG WT treated with 2 µg/mL GA (**Figure 7B**). Immunoprecipitation showed that after inhibition by GA, multiubiquitination and subsequent degradation was increased which indicates that the hERG protein is primarily consumed by the proteasome. They showed that GA prevented maturation of hERG WT channels as hERG-Hsp90 complexes could only by isolated together with core-glycosylated hERG protein after a chase of 6 hours and this formation could be inhibited by blockage of the functionally important ATPase activity of Hsp90 using GA (**Figure 7C**)[59]. Lastly, experiments were performed in ventricular cardiomyocytes from guinea pigs to determine the effects of Hsp90 inhibition on native cardiac I_{Kr} channels. Patch-clamp recordings showed that GA reduced tail current densities in guinea pig cardiomyocytes from 0.72±0.09 to 0.32±0.04 pA/pF and 0.19±0.03 pA/pF upon 24-hour exposure to 1 or 2 µg/mL GA, respectively (**Figure 7D**). This shows that, 1 µg GA applied for 24 hours reduced both native I_{Kr} currents and heterologously expressed hERG currents by about 50%. The cardiac I_{Ks} currents were not decreased by increasing concentrations of GA indicating that there is specificity in the interaction between Hsp90 and native cardiac potassium channels. As pharmacological data indicate that concentrations above 0.1 µg/ml GA are necessary to achieve antineoplastic effects[69], which is also within the range where GA inhibits hERG maturation and GA thus reduces the expression level of hERG by interfering with channel folding and maturation[59].

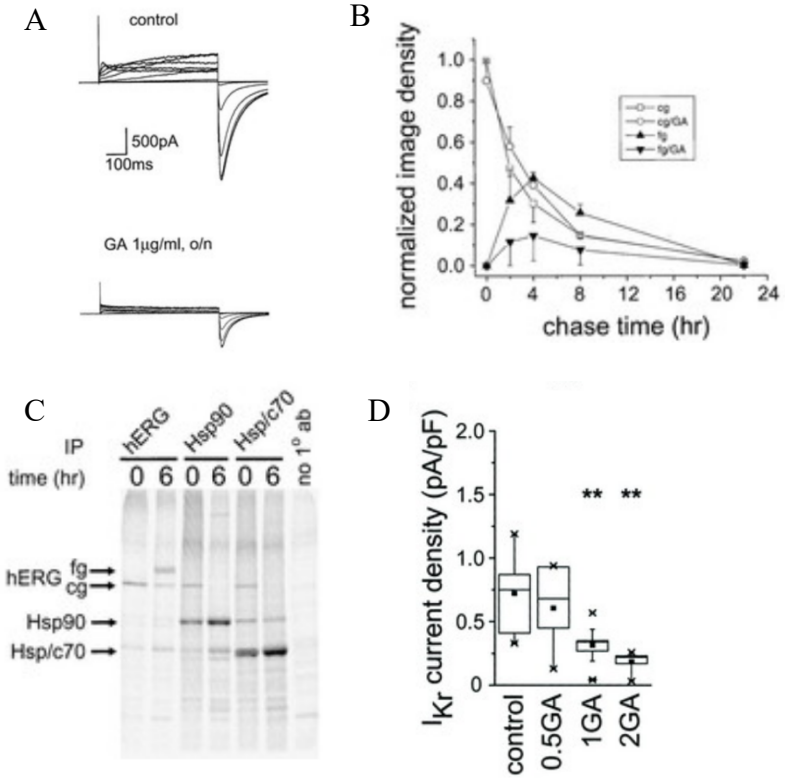

Figure 7. Graphs by *Ficker et. al*.[59] showing the effect of GA on HEK293 cells stably transfected with hERG WT and guinea pig ventricular myocytes.
A) HEK cells stably transfected with hERG WT were cultured overnight in the presence of 1 µg/mL GA and showed reduced hERG current amplitudes.
B) Pulse-chase experiments showed that in control cells, about 50% of the core-glycosylated protein (cg) of 135 kDa was converted into the mature fully glycosylated protein (fg) of 155 kDa within 4 hours, while only small amounts of fully glycosylated protein were produced in HEK293 cells stably transfected with hERG WT treated with 2 µg/mL.
C) Cross-linked samples were analyzed by immunoprecipitation after labeling (time 0) or after a 6-hour chase. Right lane represents a negative control with no primary antibody added. At t=0, radiolabeled hERG was present only in the core-glycosylated form, whereas after a 6-hour chase (t=6), both the core- and the fully glycosylated mature form were immunoprecipitated. Hsp90 and Hsp70 chaperones were isolated in complexes with the core- but not with the fully glycosylated form of the hERG channel protein.
D) Patch-clamp recordings showed that GA significantly reduced tail current densities in guinea pig cardiomyocytes from 0.72±0.09 to 0.32±0.04 pA/pF and 0.19±0.03 pA/pF upon 24-hour exposure to 1 or 2 µg/mL GA, respectively. 0.5 µg/mL GA exposure did not significantly reduce the tail current densities.

A study by *Asahi et. al.*[70] showed that 17-AAG did not inhibit hERG tail current in CHO cells overexpressing hERG (CHO-hERG cells) after exposure to 1 µM 17-AAG for 5 min, but slightly inhibited hERG tail current at 3 µM (81.0±5.2%) after exposure to 3 µM 17-AAG for 5 min. After 24 hours, a concentration-dependent decrease in hERG tail current was seen. The hERG tail current was 26.8% ± 16.8% or 21.8% ± 16.4% at 1 or 3 µM, respectively (**Figure 8A**). Furthermore, 17-AAG decreased the levels of mature hERG protein at 1 and 3 µM for 24 hours (13.9% ± 0.9% and 10.3% ± 2.1%, respectively) (**Figure 8B**). The levels of immature hERG protein were slightly decreased by 5 min of exposure to 1 and 3 µM 17-AAG (81.3% ± 7.3% and 71.1% ± 5.8%, respectively). However, the field potential (FP) assay using human embryonic stem cell-derived cardiomyocyte clusters (hES-CMs) to predict clinical QT prolongation and/or pro-arrhythmic risk[71] did not show a prolongation of field potential duration (FPD). Instead, a shortening of the FPD was observed during 2- to 24-h exposure of 1 and 3 µM 17-AAG. These results might indicate that 17-AAG also accelerate the degradation of immature hERG protein through Hsp90 inhibition and consequently decrease the expression of mature hERG channels. However, overnight exposure to GA has been reported to increase the immature hERG-Flag protein levels in hERG-HEK cells[72], while the opposite is seen for 17-AAG in hERG-CHOs[70]. This may be due to a different action of 17-AAG and further research is required to find the precise

mechanism by which 17-AAG disrupts the hERG trafficking but does not lead to prolonged QTc interval and arrhythmias[70].

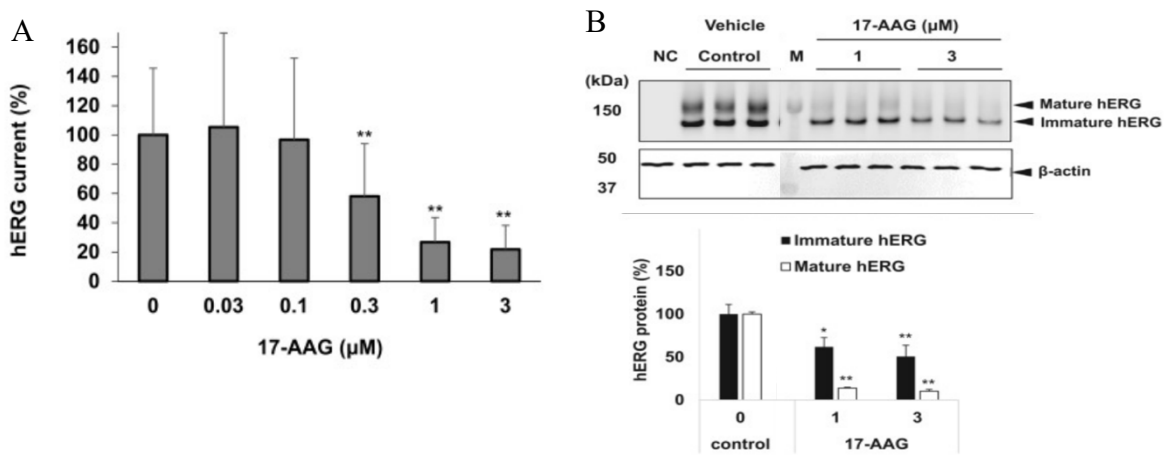

Figure 8. Graphs by *Asahi et. al*.[70] showing the effect of 17-AAG on CHO-hERG cells.
A) After 24 hours, a concentration-dependent decrease in hERG tail current was seen in CHO-hERG cells. The hERG tail current was 26.8% ± 16.8% or 21.8% ± 16.4% at 1 or 3 μM, respectively.
B) Western blots show the effects on the mature (155 kDa) or immature (135 kDa) form of hERG protein of 24 h exposure to 17-AAG. β-actin was stained as a loading control. The protein extraction of non-hERG-transfected CHO cells was loaded in the negative control (NC) lane. Size markers were loaded in the M lane. 17-AAG decreased the levels of mature hERG protein at 1 and 3 μM for 24 hours (13.9 and 10.3%, respectively)

2.4 HER2 inhibitors

Lapatinib

Lapatinib is an tyrosine kinase inhibitor used to treat solid tumors, like breast and lung cancer[73]. It inhibits the tyrosine kinase activity associated with the oncogenes encoding epidermal growth factor receptor (EGFR) and human EGFR type 2 (HER2)[74]. As the HER2 pathway is involved in cardiac function, inhibition of HER2 could cause cardiac dysfunction. Lapatinib has been associated with congestive cardiac failure, decreased left ventricular ejection fraction (LVEF) and QT prolongation[75–77]. During the clinical development program for lapatinib, cardiac events including LVEF decreases were reported in 1% of the patients[33]. Furthermore, a concentration dependent increase in QTc interval with a maximum mean of 8.75 ms was observed in a QT study in patients with advanced solid tumors. This cardiotoxicity might result from effects of lapatinib on cardiac ion channels. Blockage of one or more outward K^+ current is the most common mechanism by which drugs delay repolarization and prolong the QT interval[78].

Structure

Lapatinib is a synthetic, orally-active quinazoline and reversibly blocks the phosphorylation of EGFR, ErbB2, Erk-1 and Erk-2 kinases[79]. It is an organofluorine compound, a member of furans and a member of quinazolines. The chemical name is $C_{29}H_{26}ClFN_4O_4S$ (**Figure 9**)[80].

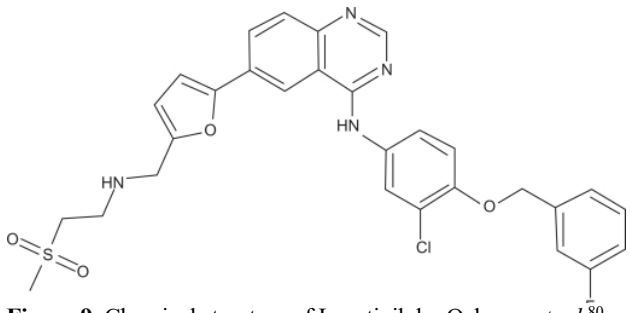

Figure 9. Chemical structure of Lapatinib by Oakman *et. al*.[80]

Mechanism of action

The molecular determinant of the hERG blockage by lapatinib is still not elucidated, so further research should unravel this mechanism.

Clinical relevance

A study by *Lee et. al.*[81] showed that 0.1, 0.3, 1.0, 3.0 and 5.0 μM lapatinib the hERG current amplitude reduced in hERG cDNA-transfected HEK293 cells (11.5±2.7, 32.9±3.5, 53.6±4.8, 71.4±2.7 and 88.5% ± 4.7, respectively) (**Figure 10A**). They determined from a non-linear fitting of the experimental hERG current values to the Hill equation, that the IC_{50} was 0.8±0.09 μM (**Figure 10B**). Furthermore, they showed the effect of lapatinib on the action potential of rabbit Purkinje fibers. Lapatinib prolonged the APD_{90} at 0.3, 1.0, 3.0 and 5.0 μM by 5.0, 7.4, 10.6 and 16.1%, respectively (**Figure 10C**). The effect was significant at 5.0 μM with a reduction of APD_{90} from 243.1±8.5 ms to 268.7±9.1 ms (**Figure 10D**). However, no effect was seen by lapatinib on the APD_{50}, resting membrane potential, total amplitude, or maximum velocity values. The administration of a single 250-mg oral dose of lapatinib yields a mean maximum concentration of lapatinib in plasma of 0.53 μM and this shows that the IC50 value obtained in their study was physiologically relevant[82]. A study by *Ando et. al.* [83], also showed in *in vivo* canine models that 3 mg/kg lapatinib administered intravenously over 10 minutes, significantly increased the QT interval, the corrected QT interval, the sinus rhythm, the pacing cycle length of 400 ms and the effective refractory period. The clinically recommended oral dose of lapatinib is 1250 mg, which produces a steady state geometric mean of 2430 ng/mL[84] and the peak plasma concentrations for 3 mg/kg lapatinib was 2358±424 ng/mL, indicating that this dosage is therapeutically relevant[83]. However, the terminal repolarization period and the beat-to-beat variability were minimally altered, which suggests that the proarrhythmic potential of lapatinib might not be serious to induce lethal ventricular arrhythmias[83]. Even though lapatinib may not induce TdP, when combining this drug with other drugs that may target the hERG channel, careful monitoring should be performed to detect cardiovascular adverse events.

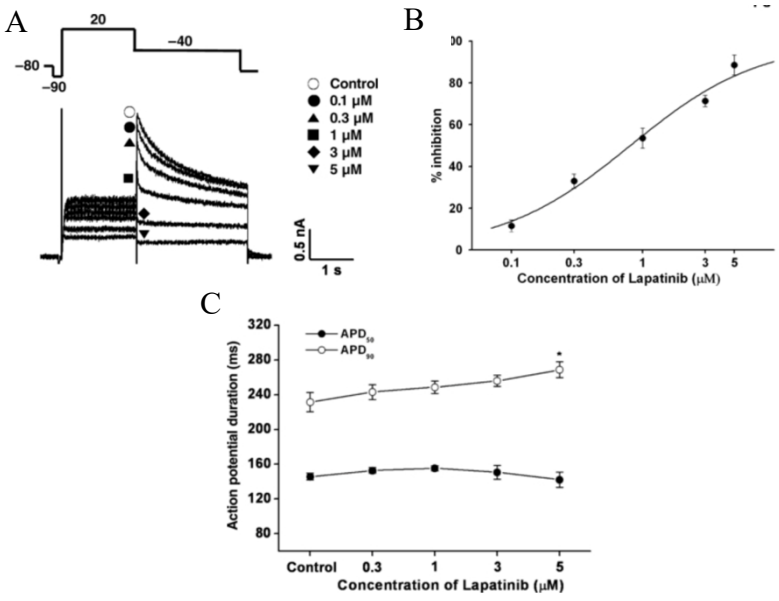

Figure 10. Graphs by *Lee et. al.*[81] showing the effect of lapatinib on HEK293 cells stably transfected with hERG and on rabbit Purkinje fibers.
A) 0.1, 0.3, 1.0, 3.0 and 5.0 μM lapatinib the hERG current amplitude reduced in hERG cDNA-transfected HEK293 cells.
B) The concentration-response relationship showed an IC_{50} of 0.8 for lapatinib block of hERG current in HEK293 stably transfected with hERG.
C) 5.0 μM lapatinib reduced the APD_{90} of rabbit Purkinje fibers from 243.1 ms to 268.7 ms. The APD_{50} is represented as closed circles and the APD_{90} as open circles.

2.5 Tyrosine Kinase Inhibitors

Crizotinib

Crizotinib is used to treat advanced non-small cell lung cancer (NSCLC). Patients with NSCLC have few effective treatment options. Standard chemotherapy only shrinks tumors in one third of the patients and only some patients have a specific mutated form of the EGFR gene that benefit from targeted therapies[85]. However, a gene mutation consisting of the fusion of the genes *EML4* and *ALK* was found to drive tumor growth and crizotinib targets this aberrant anaplastic lymphoma kinase (ALK) protein[86]. More than 10% of the patients treated with crizotinib have experienced bradycardia and 1 – 10% of the patients treated with crizotinib have experienced heart failure (sometimes with fatal outcome) and QT prolongation[87,88]. These adverse effects might indicate that crizotinib targets the hERG channel.

Structure

Crizotinib is an aminopyridine-based inhibitor of the receptor tyrosine kinase ALK and the c-Met/hepatocyte GFR (HGFR)[89]. Crizotinib binds to and inhibits ALK kinase and ALK fusion proteins in an ATP-competitive manner. It is a 3-[1-(2,6-dichloro-3-fluorophenyl)ethoxy]-5-[1-(piperidin-4-yl)pyrazol-4-yl]pyridin-2-amine with R configuration at the chiral center with the chemical name $C_{21}H_{22}Cl_2FN_5O$ (**Figure 11**)[90].

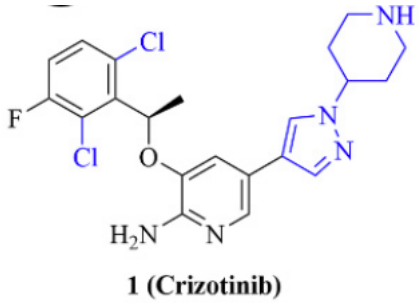

Figure 11. Chemical structure of crizotinib by *Liang et al.*[90]

Mechanism of action

The molecular determinant of the hERG block by crizotinib and in which state the hERG channel is blocked is still not elucidated, so further research should be performed to unravel this mechanism.

Clinical relevance

Crizotinib showed to inhibit the I_{Kr} channel with an IC_{50} of 1.1 µM at all concentrations tested in multiple *in vitro* studies and in a single dose *in vivo* study in anesthetized dogs[91]. These values were below or similar to the maximum blood concentrations (Cmax) seen in humans at clinically relevant doses[92]. In a 13-week dog study, males were treated with ≥ 100 mg/m^2 crizotinib and females were treated with 500 mg/m^2 crizotinib. Both showed increases in QT/QTc intervals at both week 6 and 13 pre-dose time-points compared to pretreatment[91]. These findings were consistent with increases in QT/QTc intervals observed in a one-month dog study[91]. Furthermore, a study by *Doherty et. al.*[93] showed that human induced pluripotent stem cell-derived (iPS) cardiomyocytes rapidly lost all synchronous contractions with 10 µM crizotinib, while 625 nM crizotinib induced an elongated beat pattern from 2 to 48 hours (**Figure 12A**). Normalized beat rate (NBR) was also decreased upon 625 nM crizotinib within 2 hours, and this continued in a dose- and time-dependent manner (**Figure 12B**). Furthermore, patch clamp studies performed in HEK293 cells stably infected with hERG showed that crizotinib had a IC_{50} of 1.7 µM, indicating that crizotinib potentially blocks the hERG channel[93]. As this toxicity is seen near the Cmax range of crizotinib (0.73 – 1.06 µM), the potential hERG channel block takes place at clinically relevant concentrations[92].

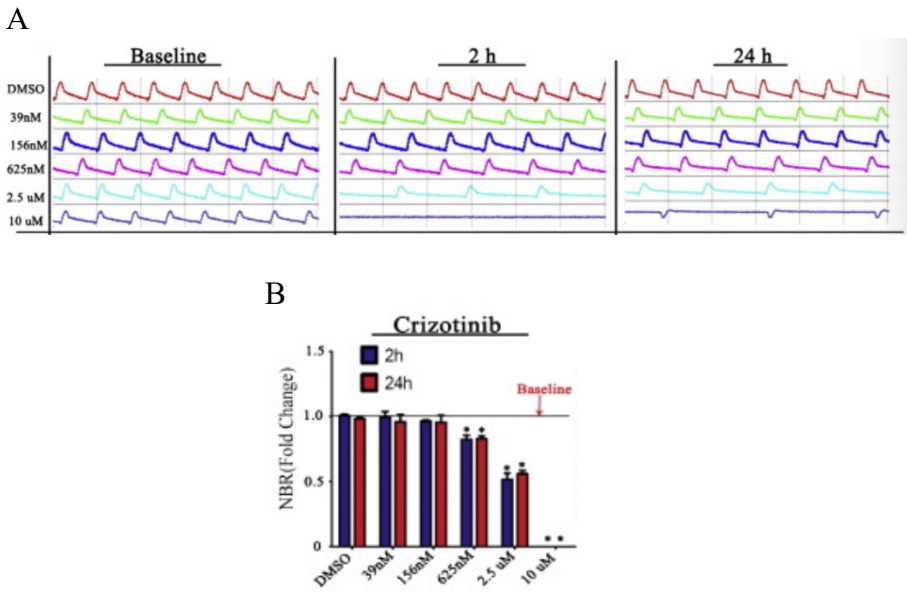

Figure 12. Graphs by *Doherty et. al*.[93] showing the effect of crizotinib on iPS-cardiomyocytes and HEK293 cells stably transfected with hERG.
A) Cardiomyocytes were dosed with DMSO or a wide dose range (39 nM–10 μM) of crizotinib and impedance measurements were recorded following treatment. Representative traces shown are approximately 11 s in duration and depict beat patterns at baseline (prior to dosing), 2 h post-treatment, and 24 h post-treatment. Rapid loss of all synchronous contractions was observed with 10 μM crizotinib
B) Normalized beat rate (NBR) data were calculated as the number of positive peaks during treatment time relative to the number of positive peaks at a time point prior to drug treatment and 625 nM crizotinib induced an elongated beat pattern from 2 to 48 hours.

Imatinib

Imatinib mesylate (IM) is a tyrosine kinase inhibitor used to manage and treat chronic myelogenous leukemia (CML), gastrointestinal stromal tumors and other malignancies[94]. CML is caused by a reciprocal translocation between chromosomes 9 and 22 resulting in *BCR-ABL* fusion gene[95]. IM binds closely to the ATP binding site of the tyrosine kinase, which inhibits the enzyme activity resulting in less downstream signaling pathways that promote leukemogenesis[96]. However, IM is associated with left ventricular dysfunction, congestive heart failure and IM induces *in vitro* significant cell apoptosis and death in isolated cardiomyocytes[97]. 0.1 – 1% of the patients treated with imatinib experienced palpitations, tachycardia or congestive heart failure[98]. HERG channels could be a target of IM as they are highly expressed in leukemia cells[99]. Off-target effects in other organs, such as the heart, might be the cause of the cardiotoxicity reported for IM.

Structure

IM is a benzamide created by formal condensation of the carboxy group of 4-[(4-methylpiperazin-1-yl)methyl]benzoic acid with the primary aromatic amino group of 4-methyl-N(3)-[4-(pyridin-3-yl)pyrimidin-2-yl]benzene-1,3-diamine[100]. It is a N-methylpiperazine, a member of benzadimes, pyridines and pyrimidines and an aromatic amine with the chemical name $C_{29}H_{31}N_7O$ (**Figure 13**)[101].

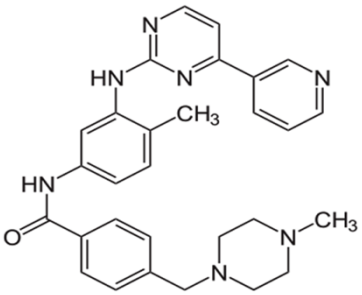

Figure 13. Chemical structure of Imatinib mesylate by *Kadivar et. al*.[101]

Mechanism of action

IM blocks the hERG channel when the channels are in an open state, but not in an inactivated state indicating that IM blocks the hERG channel in a state-dependent manner[102]. IM binds to the aromatic residues F656 and Y652 located in the S6 pore domain of the hERG channel as 100 µmol/L IM produced markedly less inhibition of the mutant Y652A and F656A channels compared to the WT hERG channels in *Xenopus* oocytes. As the inhibitory effect of IM could be reversed for 70% after 10 min of washout and IM only blocks hERG in an open state, IM is most likely not trapped by hERG during inactivation of the channel[102].

Clinical relevance

A study by *Dong et. al.*[102] showed a concentration-dependent inhibition of the peak tail current after 3, 10, 30 and 100 µmol/L IM in HEK293 cells stably transfected with WT hERG (**Figure 14A**). A nonlinear least-squares fit of concentration-response plotted using the Hill equation showed an IC_{50} of 19.51±2.50 µmol/L. 30 µmol/L IM applied to a bath solution caused a steady-state inhibition after 4-5 min. Furthermore, voltage-dependent effects of IM on hERG were investigated and the percentage of inhibition gradually increased at voltages from -40 to +60 mV and reached a steady state at +20 mV (**Figure 14B**). This indicates that blockage of hERG currents by IM increases with increasing depolarization and saturated at voltages where hERG activation is maximal. These results are in line with open-channel blockage. IM also produced a leftward shift in the midpoint of activation ($V_{1/2}$), suggesting that IM affects the activating gating of the hERG channel (**Figure 14C**). This indicates that IM preferentially binds to the channel in an open state and thus limiting a hERG conductance increase at greater depolarized potentials. On the other hand, the effect of IM on the inactivation of the hERG channels was assessed and ($V_{1/2}$) was not significantly altered by 30 µmol/L IM indicating that the voltage dependence of steady-state inactivation of hERG channels was not modified by IM. Lastly, the time course for the hERG current block by IM was assessed using an envelope of tails protocol in *Xenopus* oocytes (**Figure 14D**). The hERG current blockage at 100 µmol/L IM with brief depolarization was lower compared to a longer duration pulse. This indicates that the blockage was enhanced by further activation of the hERG current, and this is concordant with IM being able to move the channel to the open-state[102]. As the clinically relevant plasma dosing of IM range between 4.4 and 7.5 µmol/L[103,104] and the IC_{50} values were around 20 µmol/L in HEk293 cells, the blockage of the hERG channels by IM take place closely to the range of the therapeutic plasma concentration and the hERG inhibition by IM may thus be clinically relevant[102].

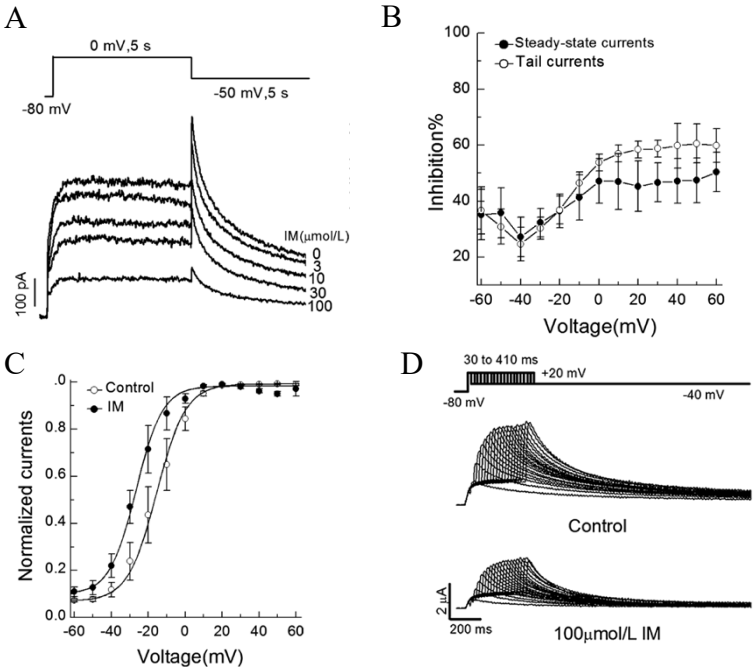

Figure 14. Graphs by *Dong et. al*.[102] showing the effect of IM on HEK293 cells stably transfected with WT hERG and *Xenopus* oocytes.
A) A concentration-dependent inhibition of the peak tail current after 3, 10, 30 and 100 μmol/L IM in HEK293 cells stably transfected with WT hERG was shown. HERG traces were elicited with 5s depolarization to 0mV from a holding potential of −80mV, and the tail current was recorded at −50mV for 5 s in the absence and presence of 3, 10, 30, and 100μmol/L IM.
B) Mean data of the voltage dependence of IM block, defined as the amplitude of current reduced by drug divided by control current amplitude, of hERG steady-state currents (closed circle) and tail currents (open circle)
C) IM produced a leftward shift in the midpoint of activation ($V_{1/2}$) in HEK293 cells stably transfected with WT hERG. The value of $V_{1/2}$ was −15.48 mV in the control sample, while the value of $V_{1/2}$ was −26.66 mV in the IM sample.
D*)* The time course for the hERG current block by IM was assessed using an envelope of tails protocol in *Xenopus* oocytes. Cells were held at −80mV and stepped to +20mV for 30 – 410 ms in 20 ms interval and then tail currents were evoked on repolarization to −40mV.

Other Tyrosine Kinase Inhibitors

Vandetanib targets vascular endothelial growth factor receptor 2, epidermal growth factor receptor (EGFR) and the proto-oncogene protein RET and is used to treat metastatic or locally advanced medullary thyroid cancer[105,106]. However, it prolonged the APD50 in rabbit Purkinje fiber at 3 μM vandetanib with 38.9% increase and the APD90 was prolonged at 1 and 3 μM vandetanib with 31 and 55.6% increase, respectively[105]. In HEK293 cells, vandetanib reduced the hERG current with an IC_{50} of 1.15±0.02 μM.

Gefitinib is an EGFR inhibitor, and it inhibits the EGFR tyrosine kinase by binding to the ATP-binding domain of the enzyme resulting in the inhibition of the anti-apoptotic Ras signaling cascade and eventually the inhibiting of cancer cells[107]. It is used to treat patients with locally advanced or metastatic non-small lung cancer (NSCLC). Gefitinib binds to the open and closed hERG channels in a concentration-dependent manner with an IC_{50} of 1.91 μM[108]. It accelerated hERG channel inactivation and decreased steady-state inactivation. Furthermore, 1 – 30 μM gefitinib increased the APD in guinea pig ventricular myocytes and the QTc in isolated perfused guinea pig hearts in a concentration-dependent manner.

Furthermore, TKI's such as bosutinib (IC_{50} = 0.3-0.7 μM), nilotinib (IC_{50} = 0.13 μM), sorafenib (IC_{50} = >3 μM), sunitinib (IC_{50} = 0.266 μM) and vemurafenib (IC_{50} = 1.24 μM) also showed inhibitory effects on the hERG channel and showed evidence for an effect on the QTc interval[109]. This indicates that although the development of TKI's have been a major breakthrough in the cancer treatment, most also show serious cardiotoxicities.

2.6 H1-receptor antagonists

Terfenadine

Terfenadine is a histamine H1-receptor blocker, which was used to treat allergies[110]. However, terfenadine has also been studied in anticancer activities as histamine has been documented to regulate cancer cell proliferation and metastasis[111]. Terfenadine has been demonstrated to exert growth-inhibitory effects and apoptotic activity against neoplastic mast cells, melanoma cells, T-cell acute lymphoblastic leukemia and prostate cancers[111–114]. Terfenadine undergoes extensive first-pass metabolism to produce an active acidic metabolite called fexofenadine, which has been shown to have no significant effect on heart rate, QT interval and to have no adverse cardiovascular safety profile[115]. However, overdosage or impaired metabolism of terfenadine resulted in QT-interval prolongation, TdP ventricular arrhythmias, and sudden death[116,117].

Structure

Terfenadine is a diarylmethane that is metabolized by intestinal CYP3A4 to the active form fexofenadine[118]. Fexofenadine competitively binds peripheral H1-receptors, stabilizing an inactive conformation of the receptor. The chemical name of Terfenadine is $C_{32}H_{41}NO_2$ (**Figure 15A**)[119]. Fexofenadine is a second-generation, long-lasting selective histamine H1 receptor antagonist[120]. It is a piperidine-based anti-histamine compound with the chemical name $C_{32}H_{39}O_4$ (**Figure 15B**)[121].

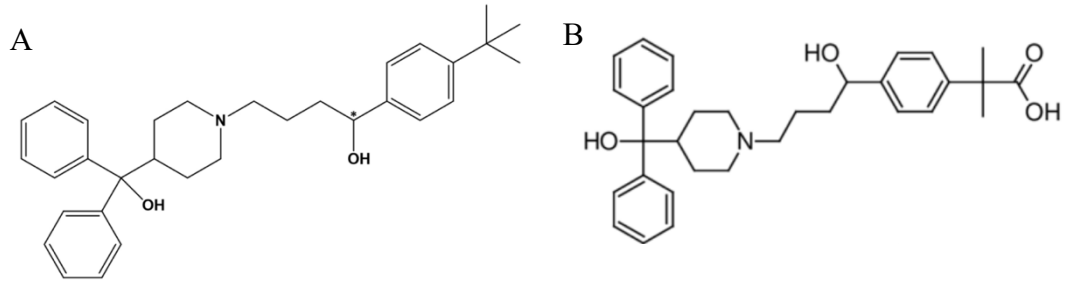

Figure 15. Chemical structures of **A**) terfenadine by *Bookwala et. al.*[119] and **B**) fexofenadine by *Vaghela et. al.*[121]

Mechanism of action

Terfenadine preferentially binds to the inactivated state of the hERG channel and both the onset of the block and recovery from the block are slow, indicating that terfenadine is trapped inside the pore when the activation gate is shut, prolonging the block[122]. Terfenadine interacts with the aromatic residues F656 and Y652 located in the S6 domain and with S624 and T623, which are located at the base of the pore helix[110]. A docking model predicts that the piperidine N and the two hydroxyl groups of terfenadine are located nearest the propeller-shaped hydrophilic space formed by the intracellular base of the pore helix and selectivity filter, where a hydrogen bond is formed to the side chain of S624[123]. The model also predicts two T-shaped π-π interactions with two Y652 and two F656 residues and two additional hydrophobic interactions with Y652 in the homotetrameric hERG channel. *Rampe et. al.*[124] showed that fexofenadine does not target the hERG channel[124].

Clinical relevance

A study by *Roy et. al.*[125] showed that 2 μmol/L terfenadine blocked the steady-state maximum current at 0 mV by 65% in *Xenopus* oocytes (**Figure 16A and B**). This block was dose dependent and equally potent on the maximal steady-state and tail currents. The binding affinity values (K_d) were 350 and 391 nmol/L, respectively (**Figure 16C**). The block of hERG current reached a steady-state level within 7 minutes after superfusion with 3 mL/min Ringer's solution containing terfenadine. The dose-response curves showed a saturation of the block for concentrations >100 μmol/L. No use-dependent, voltage-dependent, or gating-dependent block was observed indicating that terfenadine primarily produced a tonic block in the resting state. The bell-shaped I/V of hERG spreads from -40 to +40 mV, which encompasses the action potential plateau. Low doses of terfenadine will therefore introduce a regional decrease of repolarizing outward current through the primary blockage of hERG. As the highest clinical

concentration of terfenadine in human plasma was reported to be 100 nmol/L[126], the terfenadine K_d value of 350 nmol/L seems to be physiologically relevant[125].

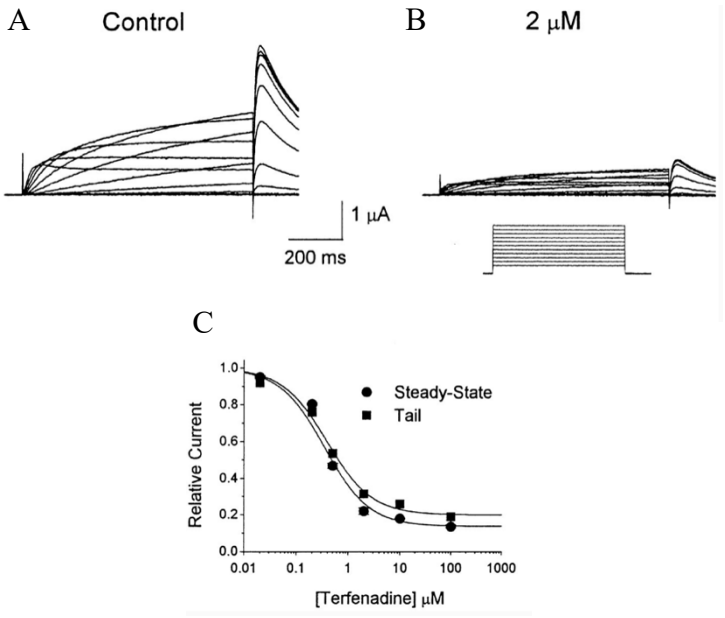

Figure 16. Graphs by *Roy et. al.*[125] showing the effect of terfenadine on *Xenopus* oocytes.
A) Control current recordings from a holding potential of −80 mV and step pulses from −60 to +40 mV in 10-mV increments in *Xenopus* oocytes.
B) 2 μmol/L terfenadine reduced both the steady-state and tail currents and the steady-state maximum current was blocked at 0 mV by 65% in *Xenopus* oocytes.
C) Dose-response curves for steady-state and tail hERG currents, generated K_d values of 350 and 391 nmol/L, respectively.

Other H1-receptor antagonists

Loratadine and astemizole are also associated as potent anti-cancer drugs, as loratadine associated with improved tumor-specific survival for immunogenic tumors and astemizole has been found to arrest the proliferation of PRC2-driven lymphomas[127,128]. However, both have also been shown to block the hERG channel after they have been associated with QT prolongation and ventricular arrhythmias[129]. Loratadine has been shown to block the hERG current amplitude with a mean IC_{50} of 173 nM[116], whereas astemizole blocked the hERG current with a half-maximal block of 0.9 nM[130].

2.7 Macrolides

Erythromycin

Erythromycin (EM) is a macrolide antibiotic, but also has shown to exert antineoplastic activities. EM has been reported to suppress NF-κB and AP-1 transcriptional activity and decrease intestinal tumorigenesis in mice, which indicates that EM can be useful as a chemoprotective agent[131]. Furthermore, EM inhibits the proliferation and induces apoptosis of cancer cells with high hERG channel expression, and it induced leukemia cell death in both myeloid and lymphoid cells by modulating the autophagic flux through inhibition of hERG1 potassium channels[131,132]. However, EM has also been reported to cause QT prolongation and torsade de points in humans, which might be indicating that EM not only inhibits hERG in cancer cells but also in ventricular myocytes[133–135].

Structure

Erythromycin is a broad-spectrum, macrolide antibiotic with antibacterial activity[136]. The bacteriostatic antibiotic drug is produced by a strain of *Saccaropolyspora erythraea* with the chemical name $C_{37}H_{67}NO_{13}$ (**Figure 17**)[137,138].

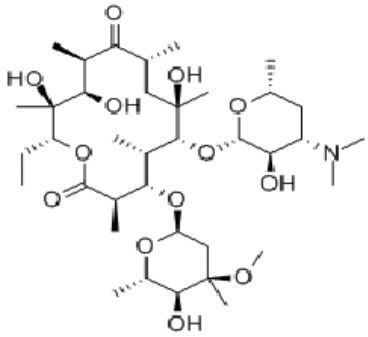

Figure 17. Chemical structure of erythromycin by *Winnicka et. al.*[138]

Mechanism of action

The blockage of the hERG channel by EM takes place during the open state of the hERG[139]. EM is unlikely to fit inside the channel's inner cavity as the structure of EM is very bulky, so the blockage with the inactivated or closed channel is highly unlikely. The aromatic residue F656 is accessible to EM when the channel is in the open state and shown to play a role in the inhibition of hERG by EM. *Guo et. al.*[140] showed that the F656 residue was a critically determinant of the temperature-dependent block of the hERG current by EM, while *Duncan et. al.*[139] found that the blockage is only partially dependent on this residue. *Duncan et. al.*[139] could not explain the found discrepancy, but they thought it might had to do something with the marked current run-up used in the sample by *Guo et. al.*[140]. The block is not significantly dependent on the Y652 residue[139].

Clinical relevance

A study by *Daleau et. al.*[141] showed that 10^{-4} mol/L EM caused a significant increase in $MAPD_{90}$ of 40±7 ms in isolated, buffer-perfused guinea pig hearts. The effects of EM were time-related and fully reversible upon removal of the drug. The effect of EM on the observed $MAPD_{90}$ was observed at a concentration of 10^{-4} mol/L or 75 mg/L EM, which is in line with the concentration reached during rapid intravenous injection of 1g EM in humans[142]. Furthermore, most EM-induced TdP cases have been observed after rapid intravenous injection of 1 g EM every 6 hours[134] or 1 g EM thrice a day over 90 minutes[133]. Additionally, 10^{-4} mol/L EM decreased the time-dependent outward K^+ current elicited by short depolarizations (250 ms) to low depolarizing voltages (-20 to 0 mV) in isolated guinea pig ventricular myocytes. This outward time-dependent K^+ current had characteristics similar to I_{Kr} and the selective block of this current explains the effects of EM on cardiac repolarization[141].

These effects of EM on cardiac repolarization were also seen in a study by *Stanat et. al.*[143]. They showed a concentration-dependent reduction in the hERG current in HEK293 cells stably transfected with hERG in the presence of 25 and 250 μM EM (**Figure 18A**). The higher drug concentration produced an increased inhibition of the evoked current, as well as the induction of a time dependent block during a depolarization step. The concentration-effect relationship was fitted with an IC_{50} of 38.9±1.2 μM. 25, 40 or 250 μM EM significantly reduced the current integral of a voltage protocol mimicking the time course of the hERG current evoked by a cardiac action potential *in vivo* (**Figure 18B**). Furthermore, the percentage of block was significantly smaller at -20 mV compared to the level of block at +60 mV with 250 μM EM. However, at voltages where hERG channel activation becomes maximal, the level of channel blockage was not significantly voltage dependent. As less blockage was observed with less positive voltages, EM may bind to open channels with rate constants that are not markedly voltage dependent. Serum concentrations of 41 μM EM have been documented after intravenous administration of 900 mg EM[142]. *Stanat et. al.*[143] found an IC_{50} of 38.9 μM for EM-induced blockage of hERG tail currents and even 25 μM EM produced a significant reduction in the total current evoked by a simulated action potential, which indicates that plasma concentrations of EM commonly achieved by intravenous administration will also produce a significant blockage of the hERG channels[143].

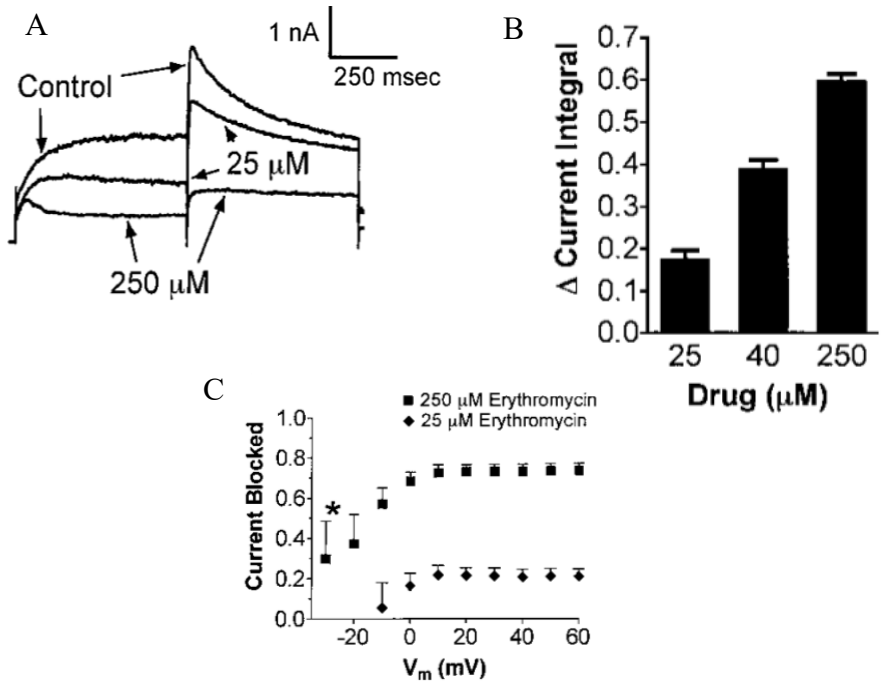

Figure 18. Graphs by *Stanat et. al*.[144] showing the effect of EM on HEK293 cells stably transfected with hERG
A) A concentration-dependent reduction in the hERG current in HEK293 cells stably transfected with hERG in the presence of 25 and 250 μM EM. 500 ms step depolarization to +10 mV activated the hERG current, after which a 500 ms step to -40 mV invoked a tail current.
B) Mean reductions in current integral for 25, 50 and 250 μM EM.
C) The voltage dependent block of EM was significantly smaller at -20 mV compared to the level of block at +60 mV with 250 μM EM.

Other macrolides

The macrolides clarithromycin and roxithromycin have been reported to cause QT prolongation and ventricular arrhythmias and they showed a concentration-dependent inhibition of the hERG current with an IC_{50} of 32.9 mM and 36.5 μM, respectively[144]. Both have also shown antitumor effects in *in vitro* studies. Clarithromycin has been shown to regulate autophagy, which sustains cell survival and resistance to chemotherapy in cancer[145]. It inhibits the growth of human colorectal cancer cells by affecting the autophagic flux and triggering apoptosis. Clarithromycin binds to the hERG channels thereby impairing the signaling pathway linking hERG and PI3K[145]. Roxithromycin reduced the tumor size of mouse B16BL6 melanoma cells and significantly inhibited pulmonary metastasis of B16BL6 cells indicating that roxithromycin has potent antiangiogenic and antitumor effects[146].

2.8 Hormone therapy

Tamoxifen and endoxifen

Tamoxifen (TAM) is nonsteroidal antiestrogen commonly used to treat estrogen-dependent breast cancer[147]. TAM competes with 17β-estradiol (E_2) at the receptor binding site and blocks the promotional role of E_2 in breast cancer[148]. However, TAM is associated with QT interval prolongation and TdP[149,150]. TAM undergoes extensive hepatic metabolism in humans by the cytochrome P450 enzyme system into several metabolites including endoxifen (END)[151]. Endoxifen is the most active metabolite of TAM and binds about 100 times more strongly to the estrogen receptor than TAM[152,153]. As END is the metabolite of TAM and TAM is associated with QT interval prolongation and TdP, END might also show cardiotoxicity.

Structure

Tamoxifen is a nonsteroidal antiestrogen and a tertiary amino compound derived from a hydride of a stilbene[154]. The chemical name of tamoxifen is $C_{26}H_{29}NO$ (**Figure 19A**)[155]. Endoxifen is also called 4-

Hydroxy-N-desmethyltamoxifen and a stilbenoid[156]. The chemical name is $C_{25}H_{27}NO_2$ (**Figure 19B**)[157].

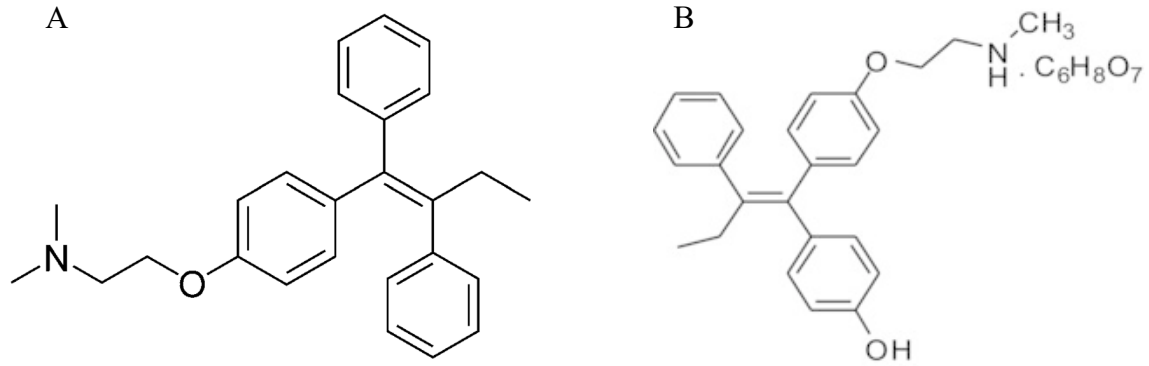

Figure 19. Chemical structures of **A**) tamoxifen by *Filippis et. al.*[156] and **B**) endoxifen by *Ahmad et. al.*[158]

Mechanism of action

TAM blocks the hERG channel in the open and/or inactivated state, whereas closed state block is minimal[158]. As the binding site is only accessible for TAM when the channel is in the open or inactivated state, it is likely that mainly open channels are blocked by tamoxifen. Furthermore, unblocking is very slowly, which might indicate that TAM is trapped in the channel after inactivation. END has shown to block the hERG channel in both the open and inactivated states and the inhibition was reversible, indicating that END might not be trapped after inactivation of the channel[159]. However, the molecular determinants of the hERG blockage by both drugs is still not elucidated. Furthermore, both TAM and END also inhibit the trafficking of the hERG channel protein to the plasma membrane, indicating that TAM and END inhibit the hERG channel currents in two ways[159]. As it is not elucidated how the drugs exactly inhibit either the direct blockage or the channel trafficking, further research is necessary to unravel the mechanism of actions of the hERG current inhibition by TAM and END.

Clinical relevance

A study by *Thomas et. al.*[158] showed that 10 and 100 µM TAM inhibited the hERG tail currents in *Xenopus laevis* oocytes and the IC_{50} for block of tail currents was 45.3 µM (**Figure 20A and B**). The onset was fast as the hERG channel block occurred within 9 minutes after addition of 100 µM TAM. The blocking effect was partially reversible within 20 minutes of washout. The hERG current voltage relationship showed that the peak tail currents were blocked by 56.8±14.2% after exposure to 50 µM TAM (**Figure 20C**). Only minimal changes in the time constant for hERG channel inactivation were observed with 50 µM TAM. A wash in of 100 µM TAM for 30 minutes caused a time-dependent increase of block to about 60% at 1000 ms (**Figure 20D**). This is in line with a very fast block of the open or inactivated hERG channels. In *Xenopus* oocyte expression systems, higher concentrations for drugs are necessary than for mammalian HEK293 cells, which is also shown by *Liu et. al.*[160] who found an IC_{50} value between 1 and 3.3 µM TAM in mammalian cardiomyocytes. TAM plasma levels are between 0.54 and 2.0 µM during breast cancer treatment[161,162] and during high-dose therapy, the concentrations have been reported to reach up to 1.56-7.0 µM TAM[163,164]. This is in line with the IC_{50} found for the blockage of hERG by TAM[160], indicating that the inhibition of the hERG channel by TAM might be of physiological relevance.

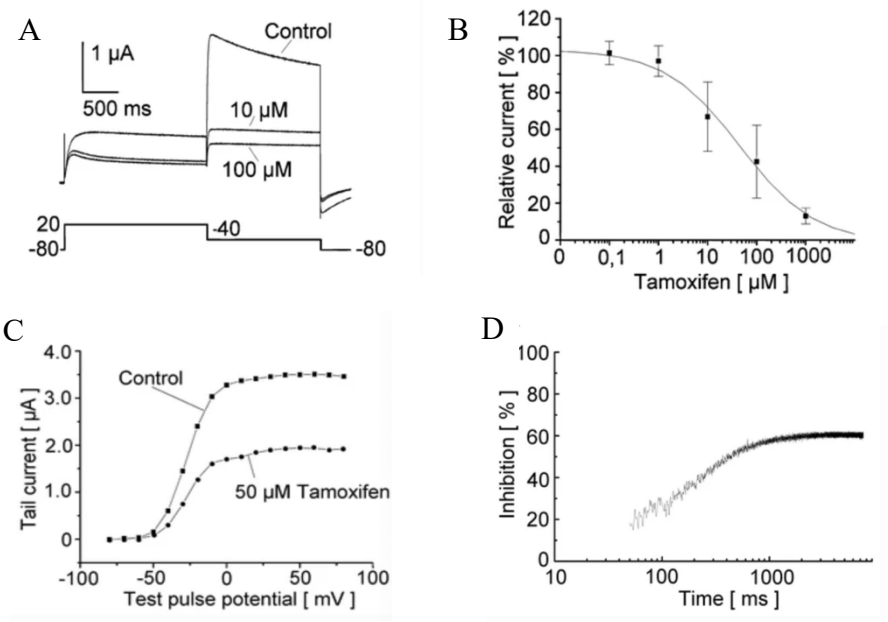

Figure 20. Graphs by *Thomas et. al.*[159] showing the effect of TAM on *Xenopus laevis* oocytes.
A) Current traces were recorded under control conditions and an inhibition was recorded after superfusion with 10 and 100 µM TAM. The currents were elicited by a depolarizing pulse to +20 mV. Tail currents were recorded during a step to -40 mV.
B) The concentration-response curve on the hERG peak tail currents showed an IC_{50} of 45.3 µM.
C) Peak tail currents were blocked by 56.82% after exposure to 50 µM TAM.
D) 100 µM TAM caused a time-dependent increase of block to about 60% at 1000 ms on a logarithmic scale.

A study by *Chae et. al.*[159] showed that 0.3, 1.3, 10 µM END inhibited hERG tail currents in a concentration-dependent manner at -50 mV with an IC_{50} of 1.6±0.2 µM in an hERG-HEK293 recombinant cell line (**Figure 21A**). For TAM, they found an IC_{50} of 1.2±0.1 µM, which was in line with the IC_{50} found by *Liu et. al.*[160] for TAM. This indicates that both END and TAM are similar in inhibiting the hERG tail currents, The I-V relationships was determined and showed that 1 µM END reduced the hERG amplitude of all hERG currents between -50 to +60 mV (**Figure 21B**). Furthermore, END shifted the $V_{1/2}$ of the activation curve in a hyperpolarizing direction (Control: -30.1 mV, END: -34.6 mV) and the voltage-dependent inhibition of hERG increased from 21.8±2.2% at -30 mV to 39.9±1.1% at 0 mV. This indicates that END preferentially interacts with the activated state of the hERG channel. A voltage-clamp experiment showed that fast application of 0.3, 1, 3 and 10 µM END caused a rapid and reversible inhibition of the tail currents in a concentration-dependent way (**Figure 21C**). This suggest that END inhibits the hERG currents by binding to the channels when they are in the open state. On top of this, 3 and 10 µM of TAM or END showed a significant reduction in the fully glycosylated hERG channel protein, indicating that both inhibit the protein trafficking of the hERG channels (**Figure 21D**). As the plasma concentrations of TAM ranged from 0.54 to 2.0 µM and with high-dose therapy could reach up to 7.0 µM[161–164], the IC_{50} of 1.2 µM found for TAM and of 1.6 µM found for END are in a clinically relevant range of therapeutic concentrations[159].

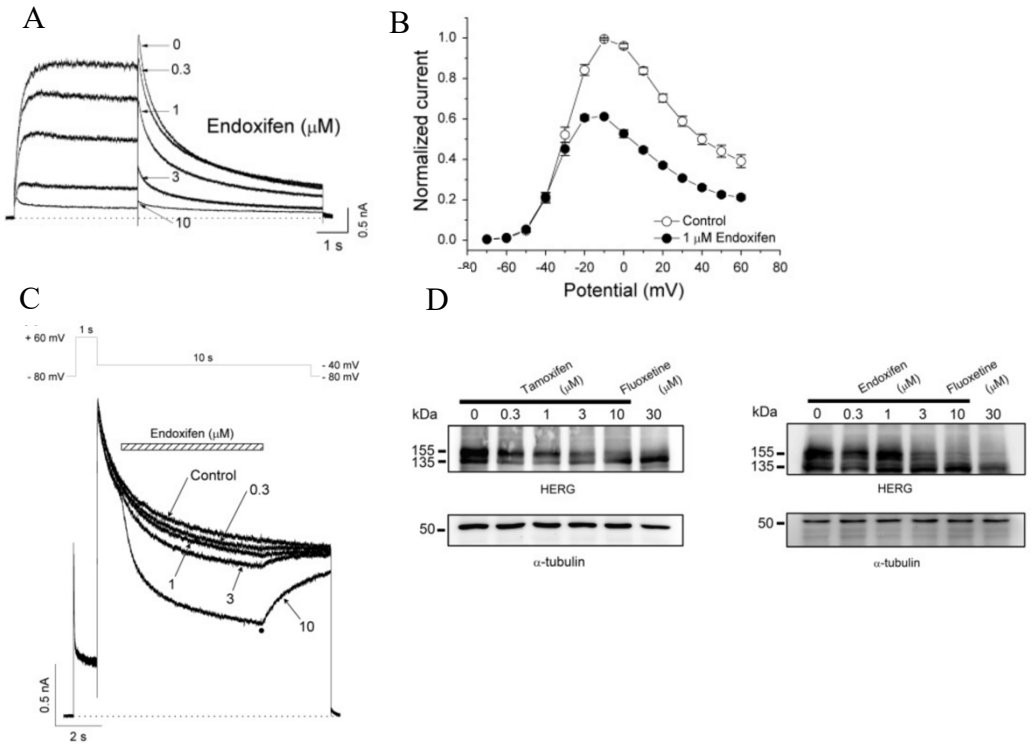

Figure 21. Graphs by *Chae et. al*.[159] showing the effects of END and/or TAM in an hERG-HEK293 recombinant cell line.
A) Whole-cell hERG currents were elicited by a 4-s depolarizing pulse to +20 mV from a holding potential of −80 mV every 15 s, after which repolarization took place to −50 mV for 6 s to generate hERG tail currents. 0.3, 1, 3 and 10 μM END inhibited hERG tail currents in a concentration-dependent manner at -50 mV.
B) Current–voltage relationships of the steady-state currents under control conditions and after application of END showed that 1 μM END reduced the hERG amplitude of all hERG currents between -50 to +60 mV.
C) Fast application of 0.3, 1, 3 and 10 μM END caused a rapid and reversible inhibition of the tail currents in a concentration-dependent way. The cells were depolarized to +60 mV for 1 s from a holding potential of −80 mV, followed by a repolarizing pulse to −40 mV for 10 s.
D) Immunoblotting showed that 3 and 10 μM TAM and END inhibited hERG channel protein trafficking as reduction in the band intensity was observed for the fully mature channel protein (155 kDa) for 3 and 10 μM TAM or END. This reduction in band intensity was not seen for the core-glycosylated channel protein (135 kDa). The immunoblot analysis was conducted using anti-hERG antibody. α-Tubulin was used as a loading control, and fluoxetine was used as positive control.

3. Discussion/conclusion

Over the years, tremendous progression in development of cancer treatments has taken place, which changed the view of cancer to a more chronic disease[1]. However, anticancer drugs can lead to drug induced arrhythmias by blocking the human ether-à-go-go related gene (hERG) potassium channel[9], thereby prolonging the corrected QT (QTc) interval[3]. In this review, different chemotherapeutic groups were assessed to find out what the mechanism of action of the hERG channel inhibition was. The two mechanisms to inhibit the hERG channel that came forward were either direct blockage of the hERG channel or inhibiting the trafficking of the fully glycosylated hERG channels to the cell surface[15].

Blockage of the channel was most often done by the binding of the drug to the aromatic residues F656 and Y652, which are located in the pore-S6 region of the hERG channel, although the blockage was less dependent on binding to Y652[48,66,139]. If the drug compounds were small enough, they could even be trapped inside the binding pocket after inactivation of the channel[50]. This leads to a longer inhibition which will make the patient more prone to arrhythmias. The drugs that directly bind to the hERG channel using the residues F656 and Y652 were amsacrine (m-AMSA), imatinib mesylate (IM), terfenadine and erythromycin (EM). Terfenadine also bound to the aromatic residues S624 and T623, which are located at the base of the pore helix, while erythromycin only bound to F656 as it was too bulky to fit inside the hERG pocket. M-AMSA binds to the hERG channels when they are in an open and/or inactivate state and binds to F656 and partially to Y652. IM and EM only bind to the hERG channels in an open state, but IM binds to both aromatic residues, whereas EM binds to F656 but only partially to Y652. In contrast, terfenadine only binds to the inactivated state of hERG and this compound binds to both F656 and Y652. No conclusions can be drawn from these different drug bindings. Therefore, unraveling how

these drugs bind to the hERG channel will help to make new chemotherapeutic compounds that cannot bind to the F656 and Y652 residues and thus may not block the hERG channel. Tamoxifen (TAM) and its metabolite endoxifen (END) also directly bind to the hERG channel, although its mechanism of action is not elucidated yet. As TAM binds to both the open and inactivated states of the channel and is might be trapped after inactivation, this compound shows similar characteristics to the binding of m-AMSA to the hERG channel. Therefore, it might be possible that TAM also binds to F656 and only partially to Y652 just like m-AMSA. END also binds to both the open and inactivated states of the channel, but it might not be trapped after channel inactivation. This mode of action is not seen with the other drugs, so no hypothesis can be drawn for the mode of action of hERG binding by END. As all drugs are from different chemotherapeutic groups, it indicates that the residues F656 and Y652 are a common binding site for the drugs and further research, such as structural and docking studies, should be performed to elucidate what molecules bind to these residues.

Inhibiting the trafficking of the fully glycosylated hERG channels to the cell surface was most often done by inhibiting the heat shock protein 90 (Hsp90)[39]. This protein together with Hsp70, interacts with the core-glycosylated form of the hERG channel cytosolic chaperones heat shock protein (Hsp) Hsp70 and Hsp90 interact with the core-glycosylated hERG channel, but not with the fully glycosylated, cell-surface form of hERG indicating that Hsp90 and 70 are both crucial for the maturation of hERG. The drugs that inhibit the trafficking of the hERG channel are Arsenic Trioxide, geldanamycin, tamoxifen and endoxifen. However, the drugs differently target Hsp90 as arsenic trioxide interacts with the thiol pair in the middle segment of Hsp90 leading to the inhibition of the binding of Hsp90 to the core-glycosylated form of hERG[40], while geldanamycin binds to ATP-specific binding site of Hsp90 inhibiting the ATPase cycle of Hsp90 and degradation of the Hsp90-substrates[68]. Furthermore, geldanamycin prevents the formation of the Hsp90-hERG complexes by blocking the functionally important ATPase activity of Hsp90. This prevents the maturation of the hERG channels into the fully glycosylated cell surface form, so geldanamycin increases proteasomal degradation of hERG channels and inhibits the formation of Hsp90-hERG complexes preventing the maturation of the channels[68]. How tamoxifen and endoxifen inhibit the trafficking of the hERG channels has yet to be unraveled, but Hsp90 might also play a role in this inhibition. These drugs are again from different chemotherapeutic groups and even the geldanamycin derivate 17-AAG also accelerates the degradation of immature hERG protein through Hsp90 inhibition, but does not lead to prolonged QTc interval and arrhythmias[70]. Unraveling this mechanism and what role the chemical structure plays in this, might give more answers how to design the new anticancer treatments without inducing QT prolongation and arrhytmias.

For the drugs, lapatinib, crizotinib, tamoxifen and endoxifen are the mechanism of inhibition still not elucidated. As lapatinib and crizotinib are both tyrosine kinase inhibitors (TKI's) and a lot of TKI's have been found to inhibit the hERG channel[109], elucidating the mechanism of inhibition in this chemotherapeutic group and comparing the chemical structures with each other might give more information into the mechanism of action of the inhibition. The chemical structures of lapatinib, crizotinib and imatinib are all long chains of aromatic rings, which could easily fit into the binding pocket of hERG. As imatinib mesylate has shown to bind to the F656 and/or Y652 residues, lapatinib and crizotinib may also bind to hERG in the same way due to their similar chemical structure. Further research could elucidate the specific molecules that are involved in this binding in order to design new TKI's that do not bind to the hERG channel.

Drugs that inhibit the hERG channel but have not shown to prolong the QT interval, such as 17-AAG for example, should still be carefully monitored when used as treatment as most agents will be given simultaneously and if two agents are used that both inhibit the hERG channel but not induce QT prolongation, simultaneously they could induce arrhythmias. On top of this, many cytotoxic agents, and targeted therapies for cancer treatment, also have an effect on the cardiovascular system[165]. One reason for this, is that many agents do not only target the tumor, but also reach targets in other systems, such as the heart. A patient that undergoes cancer therapy has a substantial risk for the deterioration of their cardiovascular health. If this patient is older, the chance they already have some sort of cardiovascular problems, is very high. These problems can thus be worsened by the cancer therapy, which can lead to

life-threatening situations. Agents that target the hERG channel but do not induce arrhythmias in a healthy population, could therefore induce arrhythmias in older patients.

In short, chemotherapeutic agents that cause QT prolongation and arrhythmias inhibit the hERG channel by either binding to the F656 and/or Y652 aromatic residues in the binding pocket of hERG creating a direct blockage of the channel or inhibiting the trafficking of the fully glycosylated hERG channels to the cell surface by inhibiting the hERG-Hsp90 complex formation. Further research should be performed to elucidate the exact molecules that bind to the residues in the binding pocket and new chemotherapeutic agents should be studied for Hsp90 inhibition, which may lead to hERG channel degradation. Agents that target the hERG channel but do not induce arrhythmias should still be carefully monitored in older patients as they have an increased risk of proarrhythmogenic events indicating that every new chemotherapeutic agent should be studied for their potential inhibitory effect on the hERG channel and elucidating the mechanism of the inhibition will make the development of new chemotherapeutic agents safer, even for the aging population.

4. References

1. Suter TM, Ewer MS. Cancer drugs and the heart: Importance and management. *Eur Heart J*. 2013;34(15):1102-1111. doi:10.1093/eurheartj/ehs181
2. Tamargo J, Caballero R, Delpón E. Cancer Chemotherapy and Cardiac Arrhythmias: A Review. *Drug Saf*. 2015;38(2):129-152. doi:10.1007/s40264-014-0258-4
3. Buza V, Rajagopalan B, Curtis AB. Cancer Treatment–Induced Arrhythmias. *Circ Arrhythmia Electrophysiol*. 2017;10(8). doi:10.1161/CIRCEP.117.005443
4. Alexandre J, Moslehi JJ, Bersell KR, Funck-Brentano C, Roden DM, Salem J-E. Anticancer drug-induced cardiac rhythm disorders: Current knowledge and basic underlying mechanisms. *Pharmacol Ther*. 2018;189:89-103. doi:10.1016/j.pharmthera.2018.04.009
5. Chang H-M, Okwuosa TM, Scarabelli T, Moudgil R, Yeh ETH. Cardiovascular Complications of Cancer Therapy. *J Am Coll Cardiol*. 2017;70(20):2552-2565. doi:10.1016/j.jacc.2017.09.1095
6. Chang H-M, Moudgil R, Scarabelli T, Okwuosa TM, Yeh ETH. Cardiovascular Complications of Cancer Therapy. *J Am Coll Cardiol*. 2017;70(20):2536-2551. doi:10.1016/j.jacc.2017.09.1096
7. El-Sherif N, Turitto G. Torsade de pointes. *Curr Opin Cardiol*. 2003;18(1):6-13. doi:10.1097/00001573-200301000-00002
8. Vandenberg JI, Perry MD, Perrin MJ, Mann SA, Ke Y, Hill AP. hERG K + Channels: Structure, Function, and Clinical Significance. *Physiol Rev*. 2012;92(3):1393-1478. doi:10.1152/physrev.00036.2011
9. Priest B, Bell IM, Garcia M. Role of hERG potassium channel assays in drug development. *Channels*. 2008;2(2):87-93. doi:10.4161/chan.2.2.6004
10. Gutman GA, Chandy KG, Adelman JP, et al. International Union of Pharmacology. XLI. Compendium of Voltage-Gated Ion Channels: Potassium Channels. *Pharmacol Rev*. 2003;55(4):583-586. doi:10.1124/pr.55.4.9
11. Raschi E, Vasina V, Poluzzi E, De Ponti F. The hERG K+ channel: target and antitarget strategies in drug development. *Pharmacol Res*. 2008;57(3):181-195. doi:10.1016/j.phrs.2008.01.009
12. Curran ME, Splawski I, Timothy KW, Vincen GM, Green ED, Keating MT. A molecular basis for cardiac arrhythmia: HERG mutations cause long QT syndrome. *Cell*. 1995;80(5):795-803. doi:10.1016/0092-8674(95)90358-5
13. Sanguinetti MC, Jiang C, Curran ME, Keating MT. A mechanistic link between an inherited and an acquird cardiac arrthytmia: HERG encodes the IKr potassium channel. *Cell*. 1995;81(2):299-307. doi:10.1016/0092-8674(95)90340-2
14. Anson BD, Weaver JG, Ackerman MJ, et al. Blockade of HERG channels by HIV protease inhibitors. *Lancet*. 2005;365(9460):682-686. doi:10.1016/S0140-6736(05)17950-1

15. van der Heyden MAG, Smits ME, Vos MA. Drugs and trafficking of ion channels: a new pro-arrhythmic threat on the horizon? *Br J Pharmacol*. 2008;153(3):406-409. doi:10.1038/sj.bjp.0707618
16. Recanatini M, Poluzzi E, Masetti M, Cavalli A, De Ponti F. QT prolongation through hERG K+ channel blockade: Current knowledge and strategies for the early prediction during drug development. *Med Res Rev*. 2005;25(2):133-166. doi:10.1002/med.20019
17. Jones EMC, Roti Roti EC, Wang J, Delfosse SA, Robertson GA. Cardiac IKr Channels Minimally Comprise hERG 1a and 1b Subunits. *J Biol Chem*. 2004;279(43):44690-44694. doi:10.1074/jbc.M408344200
18. He S, Moutaoufik MT, Islam S, et al. HERG channel and cancer: A mechanistic review of carcinogenic processes and therapeutic potential. *Biochim Biophys Acta - Rev Cancer*. 2020;1873(2):188355. doi:10.1016/J.BBCAN.2020.188355
19. Stansfeld PJ, Gedeck P, Gosling M, Cox B, Mitcheson JS, Sutcliffe MJ. Drug block of the hERG potassium channel: Insight from modeling. *Proteins Struct Funct Bioinforma*. 2007;68(2):568-580. doi:10.1002/prot.21400
20. Kamiya K, Niwa R, Mitcheson JS, Sanguinetti MC. Molecular Determinants of hERG Channel Block. *Mol Pharmacol*. 2006;69(5):1709-1716. doi:10.1124/mol.105.020990
21. Kamiya K, Mitcheson JS, Yasui K, Kodama I, Sanguinetti MC. Open Channel Block of HERG K + Channels by Vesnarinone. *Mol Pharmacol*. 2001;60(2):244-253. doi:10.1124/mol.60.2.244
22. Mitcheson JS, Chen J, Lin M, Culberson C, Sanguinetti MC. A structural basis for drug-induced long QT syndrome. *Proc Natl Acad Sci U S A*. 2000;97(22):12329. doi:10.1073/PNAS.210244497
23. Cabral JHM, Lee A, Cohen SL, Chait BT, Li M, Mackinnon R. Crystal Structure and Functional Analysis of the HERG Potassium Channel N Terminus. *Cell*. 1998;95(5):649-655. doi:10.1016/S0092-8674(00)81635-9
24. Warmke JW, Ganetzky B. A family of potassium channel genes related to eag in Drosophila and mammals. *Proc Natl Acad Sci*. 1994;91(8):3438-3442. doi:10.1073/pnas.91.8.3438
25. Delisle BP, Underkofler HAS, Moungey BM, et al. Small GTPase Determinants for the Golgi Processing and Plasmalemmal Expression of Human Ether-a-go-go Related (hERG) K+ Channels. *J Biol Chem*. 2009;284(5):2844-2853. doi:10.1074/jbc.M807289200
26. Zhou Z, Gong Q, Epstein ML, January CT. HERG Channel Dysfunction in Human Long QT Syndrome. *J Biol Chem*. 1998;273(33):21061-21066. doi:10.1074/jbc.273.33.21061
27. Lamothe SM, Hulbert M, Guo J, Li W, Yang T, Zhang S. Glycosylation stabilizes hERG channels on the plasma membrane by decreasing proteolytic susceptibility. *FASEB J*. 2018;32(4):1933-1943. doi:10.1096/fj.201700832R
28. Piper DR, Hinz WA, Tallurri CK, Sanguinetti MC, Tristani-Firouzi M. Regional Specificity of Human ether-a'-go-go-related Gene Channel Activation and Inactivation Gating. *J Biol Chem*. 2005;280(8):7206-7217. doi:10.1074/jbc.M411042200
29. Sanguinetti MC, Tristani-Firouzi M. hERG potassium channels and cardiac arrhythmia. *Nature*. 2006;440(7083):463-469. doi:10.1038/nature04710
30. Martyn YL, Mahaut-Smith P, Varghese A, Huang CL -H., Kemp PR, Vandenberg JI. Effects of premature stimulation on HERG K + channels. *J Physiol*. 2001;537(3):843-851. doi:10.1111/j.1469-7793.2001.00843.x
31. Drolet B, Simard C, Roden DM. Unusual Effects of a QT-Prolonging Drug, Arsenic Trioxide, on Cardiac Potassium Currents. *Circulation*. 2004;109(1):26-29. doi:10.1161/01.CIR.0000109484.00668.CE
32. arseentrioxide. https://www.farmacotherapeutischkompas.nl/bladeren/preparaatteksten/a/arseentrioxide. Accessed July 13, 2022.
33. Boiten W. Annex I. SUMMARY OF PRODUCT CHARACTERISTICS - JEVTANA. 2003.
34. Chiang C-E, Luk H-N, Wang T-M, Ding PY-A. Prolongation of cardiac repolarization by arsenic trioxide. *Blood*. 2002;100(6):2249-2252. doi:10.1182/blood-2002-02-0598
35. Pubchem. Arsenic trioxide | As2O3 - PubChem. https://pubchem.ncbi.nlm.nih.gov/compound/Arsenic-trioxide#section=Structures. Published 2021. Accessed June 22, 2022.

36. Khairul I, Wang QQ, Jiang YH, Wang C, Naranmandura H. Metabolism, toxicity and anticancer activities of arsenic compounds. *Oncotarget*. 2017;8(14):23905-23926. doi:10.18632/oncotarget.14733
37. Ficker E, Kuryshev YA, Dennis AT, et al. Mechanisms of Arsenic-Induced Prolongation of Cardiac Repolarization. *Mol Pharmacol*. 2004;66(1):33-44. doi:10.1124/mol.66.1.33
38. Wan X, Dennis AT, Obejero-Paz C, et al. Oxidative Inactivation of the Lipid Phosphatase Phosphatase and Tensin Homolog on Chromosome Ten (PTEN) as a Novel Mechanism of Acquired Long QT Syndrome. *J Biol Chem*. 2011;286(4):2843-2852. doi:10.1074/jbc.M110.125526
39. Ficker E, Dennis AT, Wang L, Brown AM. Role of the Cytosolic Chaperones Hsp70 and Hsp90 in Maturation of the Cardiac Potassium Channel hERG. *Circ Res*. 2003;92(12). doi:10.1161/01.RES.0000079028.31393.15
40. Matsumoto S, Tanaka E, Nemoto TK, et al. Interaction between the N-terminal and Middle Regions Is Essential for the in Vivo Function of HSP90 Molecular Chaperone. *J Biol Chem*. 2002;277(38):34959-34966. doi:10.1074/jbc.M203038200
41. Shen Z-X, Chen G-Q, Ni J-H, et al. Use of Arsenic Trioxide (As2O3) in the Treatment of Acute Promyelocytic Leukemia (APL): II. Clinical Efficacy and Pharmacokinetics in Relapsed Patients. *Blood*. 1997;89(9):3354-3360. doi:10.1182/blood.V89.9.3354
42. Ketron AC, Denny WA, Graves DE, Osheroff N. Amsacrine as a Topoisomerase II Poison: Importance of Drug–DNA Interactions. *Biochemistry*. 2012;51(8):1730-1739. doi:10.1021/bi201159b
43. Cassileth PA, Gale RP. Amsacrine: A review. *Leuk Res*. 1986;10(11):1257-1265. doi:10.1016/0145-2126(86)90331-0
44. Shinar E, Hasin Y. Acute electrocardiographic changes induced by amsacrine. *Cancer Treat Rep*. 1984;68(9):1169-1172. https://pubmed.ncbi.nlm.nih.gov/6592038/. Accessed June 22, 2022.
45. Weiss RB, Grillo-López AJ, Marsoni S, Posada JG, Hess F, Ross BJ. Amsacrine-associated cardiotoxicity: an analysis of 82 cases. *J Clin Oncol*. 1986;4(6):918-928. doi:10.1200/JCO.1986.4.6.918
46. FOLDES JA. Ventricular Fibrillation, Hypokalemia, and AMSA Therapy. *Ann Intern Med*. 1982;96(1):121. doi:10.7326/0003-4819-96-1-121_2
47. amsacrine. https://www.farmacotherapeutischkompas.nl/bladeren/preparaatteksten/a/amsacrine. Accessed July 13, 2022.
48. Thomas D, Hammerling BC, Wu K, et al. Inhibition of cardiac HERG currents by the DNA topoisomerase II inhibitor amsacrine: mode of action. *Br J Pharmacol*. 2004;142(3):485-494. doi:10.1038/sj.bjp.0705795
49. Amsacrine | C21H19N3O3S - PubChem. https://pubchem.ncbi.nlm.nih.gov/compound/Amsacrine. Accessed June 22, 2022.
50. Mitcheson JS, Chen J, Sanguinetti MC. Trapping of a Methanesulfonanilide by Closure of the Herg Potassium Channel Activation Gate. *J Gen Physiol*. 2000;115(3):229-240. doi:10.1085/jgp.115.3.229
51. Linder T, Bernsteiner H, Saxena P, et al. Drug trapping in hERG K + channels: (not) a matter of drug size? *Medchemcomm*. 2016;7(3):512-518. doi:10.1039/C5MD00443H
52. Jurlina JL, Varcoe AR, Paxton JW. Pharmacokinetics of amsacrine in patients receiving combined chemotherapy for treatment of acute myelogenous leukemia. *Cancer Chemother Pharmacol*. 1985;14(1):21-25. doi:10.1007/BF00552719
53. Linssen P, Brons P, Knops G, Wessels H, Witte T. Plasma and cellular pharmacokinetics of m-AMSA related to in vitro toxicity towards normal and leukemic clonogenic bone marrow cells (CFU-GM, CFU-L). *Eur J Haematol*. 2009;50(3):149-154. doi:10.1111/j.1600-0609.1993.tb00083.x
54. Neckers L. Hsp90 inhibitors as novel cancer chemotherapeutic agents. *Trends Mol Med*. 2002;8(4):S55-S61. doi:10.1016/S1471-4914(02)02316-X
55. Park J-W, Yeh MW, Wong MG, et al. The Heat Shock Protein 90-Binding Geldanamycin Inhibits Cancer Cell Proliferation, Down-Regulates Oncoproteins, and Inhibits Epidermal Growth Factor-Induced Invasion in Thyroid Cancer Cell Lines. *J Clin Endocrinol Metab*. 2003;88(7):3346-3353. doi:10.1210/jc.2002-020340

56. An WG, Schnur RC, Neckers L, Blagosklonny M V. Depletion of p185 erbB2 , Raf-1 and mutant p53 proteins by geldanamycin derivatives correlates with antiproliferative activity. *Cancer Chemother Pharmacol*. 1997;40(1):60-64. doi:10.1007/s002800050626
57. Karkoulis PK, Stravopodis DJ, Konstantakou EG, Voutsinas GE. Targeted inhibition of heat shock protein 90 disrupts multiple oncogenic signaling pathways, thus inducing cell cycle arrest and programmed cell death in human urinary bladder cancer cell lines. *Cancer Cell Int*. 2013;13(1):11. doi:10.1186/1475-2867-13-11
58. Schulte TW, Neckers LM. The benzoquinone ansamycin 17-allylamino-17-demethoxygeldanamycin binds to HSP90 and shares important biologic activities with geldanamycin. *Cancer Chemother Pharmacol*. 1998;42(4):273-279. doi:10.1007/s002800050817
59. Ficker E, Dennis AT, Wang L, Brown AM. Role of the Cytosolic Chaperones Hsp70 and Hsp90 in Maturation of the Cardiac Potassium Channel hERG. *Circ Res*. 2003;92(12). doi:10.1161/01.RES.0000079028.31393.15
60. Dennis A, Wang L, Wan X, Ficker E. hERG channel trafficking: novel targets in drug-induced long QT syndrome. *Biochem Soc Trans*. 2007;35(5):1060-1063. doi:10.1042/BST0351060
61. Neckers L, Workman P. Hsp90 Molecular Chaperone Inhibitors: Are We There Yet? *Clin Cancer Res*. 2012;18(1):64-76. doi:10.1158/1078-0432.CCR-11-1000
62. Wenkert D, Ramirez B, Shen Y, Kron MA. In Vitro Activity of Geldanamycin Derivatives against Schistosoma japonicum and Brugia malayi. *J Parasitol Res*. 2010;2010:1-7. doi:10.1155/2010/716498
63. Geldanamycin | C29H40N2O9 - PubChem. https://pubchem.ncbi.nlm.nih.gov/compound/5288382. Accessed June 27, 2022.
64. Tanespimycin | C31H43N3O8 - PubChem. https://pubchem.ncbi.nlm.nih.gov/compound/Tanespimycin. Accessed June 28, 2022.
65. Mout R, Xu Z-D, Wolf AKH, Jo Davisson V, Jarori GK. Anti-malarial activity of geldanamycin derivatives in mice infected with Plasmodium yoelii. *Malar J*. 2012;11(1):54. doi:10.1186/1475-2875-11-54
66. Stebbins CE, Russo AA, Schneider C, Rosen N, Hartl FU, Pavletich NP. Crystal Structure of an Hsp90–Geldanamycin Complex: Targeting of a Protein Chaperone by an Antitumor Agent. *Cell*. 1997;89(2):239-250. doi:10.1016/S0092-8674(00)80203-2
67. Roe SM, Prodromou C, O'Brien R, Ladbury JE, Piper PW, Pearl LH. Structural Basis for Inhibition of the Hsp90 Molecular Chaperone by the Antitumor Antibiotics Radicicol and Geldanamycin. *J Med Chem*. 1999;42(2):260-266. doi:10.1021/jm980403y
68. Grenert JP, Sullivan WP, Fadden P, et al. The Amino-terminal Domain of Heat Shock Protein 90 (hsp90) That Binds Geldanamycin Is an ATP/ADP Switch Domain That Regulates hsp90 Conformation. *J Biol Chem*. 1997;272(38):23843-23850. doi:10.1074/jbc.272.38.23843
69. Supko JG, Hickman RL, Grever MR, Malspeis L. Preclinical pharmacologic evaluation of geldanamycin as an antitumor agent. *Cancer Chemother Pharmacol*. 1995;36(4):305-315. doi:10.1007/BF00689048
70. Asahi Y, Nomura F, Abe Y, et al. Electrophysiological evaluation of pentamidine and 17-AAG in human stem cell-derived cardiomyocytes for safety assessment. *Eur J Pharmacol*. 2019;842:221-230. doi:10.1016/j.ejphar.2018.10.046
71. Kaneko T, Nomura F, Hamada T, et al. On-chip in vitro cell-network pre-clinical cardiac toxicity using spatiotemporal human cardiomyocyte measurement on a chip. *Sci Rep*. 2015;4(1):4670. doi:10.1038/srep04670
72. Iwai C, Li P, Kurata Y, et al. Hsp90 prevents interaction between CHIP and HERG proteins to facilitate maturation of wild-type and mutant HERG proteins. *Cardiovasc Res*. 2013;100(3):520-528. doi:10.1093/cvr/cvt200
73. Burris HA. Dual Kinase Inhibition in the Treatment of Breast Cancer: Initial Experience with the EGFR/ErbB-2 Inhibitor Lapatinib. *Oncologist*. 2004;9(S3):10-15. doi:10.1634/theoncologist.9-suppl_3-10
74. Montemurro F, Valabrega G, Aglietta M. Lapatinib: a dual inhibitor of EGFR and HER2 tyrosine kinase activity. *Expert Opin Biol Ther*. 2007;7(2):257-268. doi:10.1517/14712598.7.2.257
75. Perez EA, Koehler M, Byrne J, Preston AJ, Rappold E, Ewer MS. Cardiac Safety of Lapatinib:

Pooled Analysis of 3689 Patients Enrolled in Clinical Trials. *Mayo Clin Proc*. 2008;83(6):679-686. doi:10.4065/83.6.679
76. Leslie KK, Sill MW, Lankes HA, et al. Lapatinib and potential prognostic value of EGFR mutations in a Gynecologic Oncology Group phase II trial of persistent or recurrent endometrial cancer. *Gynecol Oncol*. 2012;127(2):345-350. doi:10.1016/j.ygyno.2012.07.127
77. Choi HD, Chang MJ. Cardiac toxicities of lapatinib in patients with breast cancer and other HER2-positive cancers: a meta-analysis. *Breast Cancer Res Treat*. 2017;166(3):927-936. doi:10.1007/s10549-017-4460-9
78. Jeron A, Mitchell GF, Zhou J, et al. Inducible polymorphic ventricular tachyarrhythmias in a transgenic mouse model with a long Q-T phenotype. *Am J Physiol Circ Physiol*. 2000;278(6):H1891-H1898. doi:10.1152/ajpheart.2000.278.6.H1891
79. Lapatinib | C29H26ClFN4O4S - PubChem. https://pubchem.ncbi.nlm.nih.gov/compound/Lapatinib. Accessed June 30, 2022.
80. Di Leo A. Role of lapatinib in the first-line treatment of patients with metastatic breast cancer. *Cancer Manag Res*. 2010;2(1):13. doi:10.2147/CMR.S8951
81. Lee H-A, Kim E-J, Hyun S-A, Park S-G, Kim K-S. Electrophysiological Effects of the Anti-Cancer Drug Lapatinib on Cardiac Repolarization. *Basic Clin Pharmacol Toxicol*. 2010;107(1):614-618. doi:10.1111/j.1742-7843.2010.00556.x
82. Bence AK, Anderson EB, Halepota MA, et al. Phase I pharmacokinetic studies evaluating single and multiple doses of oral GW572016, a dual EGFR-ErbB2 inhibitor, in healthy subjects. *Invest New Drugs*. 2005;23(1):39-49. doi:10.1023/B:DRUG.0000047104.45929.ea
83. Ando K, Wada T, Cao X. Precise safety pharmacology studies of lapatinib for onco-cardiology assessed using in vivo canine models. *Sci Rep*. 2020;10(1):738. doi:10.1038/s41598-020-57601-x
84. Lapatinib | C29H26ClFN4O4S - PubChem. https://pubchem.ncbi.nlm.nih.gov/compound/Lapatinib. Accessed July 1, 2022.
85. Crizotinib for Advanced Non-Small Cell Lung Cancer - National Cancer Institute. National Cancer Institute. https://www.cancer.gov/types/lung/research/crizotinib. Published 2014. Accessed July 2, 2022.
86. Soda M, Choi YL, Enomoto M, et al. Identification of the transforming EML4–ALK fusion gene in non-small-cell lung cancer. *Nature*. 2007;448(7153):561-566. doi:10.1038/nature05945
87. FDA. *CENTER FOR DRUG EVALUATION AND RESEARCH - APPLICATION NUMBER 761055Orig1s014*.; 2019. https://www.accessdata.fda.gov/drugsatfda_docs/nda/2019/761055Orig1s014rev.pdf. Accessed July 2, 2022.
88. crizotinib. https://www.farmacotherapeutischkompas.nl/bladeren/preparaatteksten/c/crizotinib. Accessed July 13, 2022.
89. PubChem. Crizotinib | C21H22Cl2FN5O - PubChem. https://pubchem.ncbi.nlm.nih.gov/compound/Crizotinib. Accessed July 4, 2022.
90. Liang Y, Fang R, Rao Q. An Insight into the Medicinal Chemistry Perspective of Macrocyclic Derivatives with Antitumor Activity: A Systematic Review. *Molecules*. 2022;27(9):2837. doi:10.3390/molecules27092837
91. Pharmacology C. Center for Drug Evaluation and Research, Application number: 208573Orig1s000. *Clin Pharmacol Biopharm Rev*. 2015:1-183.
92. Mishina E V., Gosh TK. Center for Drug Evaluation and Research Application Number: 22-512 Clinical Pharmacology and Biopharmaceutics Review. 2010.
93. Doherty KR, Wappel RL, Talbert DR, et al. Multi-parameter in vitro toxicity testing of crizotinib, sunitinib, erlotinib, and nilotinib in human cardiomyocytes. *Toxicol Appl Pharmacol*. 2013;272(1):245-255. doi:10.1016/j.taap.2013.04.027
94. Cismowski MJ. Imatinib. In: *XPharm: The Comprehensive Pharmacology Reference*. Elsevier; 2007:1-7. doi:10.1016/B978-008055232-3.61918-X
95. Deininger M, Buchdunger E, Druker BJ. The development of imatinib as a therapeutic agent for chronic myeloid leukemia. *Blood*. 2005;105(7):2640-2653. doi:10.1182/blood-2004-08-3097
96. Iqbal N, Iqbal N. Imatinib: A Breakthrough of Targeted Therapy in Cancer. *Chemother Res Pract*. 2014;2014:1-9. doi:10.1155/2014/357027

97. Kerkelä R, Grazette L, Yacobi R, et al. Cardiotoxicity of the cancer therapeutic agent imatinib mesylate. *Nat Med*. 2006;12(8):908-916. doi:10.1038/nm1446
98. imatinib. https://www.farmacotherapeutischkompas.nl/bladeren/preparaatteksten/i/imatinib. Accessed July 14, 2022.
99. Zheng F, Li H, Liang K, Du Y, Guo D, Huang S. Imatinib has the potential to exert its antileukemia effects by down-regulating hERG1 K+ channels in chronic myelogenous leukemia. *Med Oncol*. 2012;29(3):2127-2135. doi:10.1007/s12032-011-0102-y
100. Information NC for B, Medicine USNL of, Pike 8600 Rockville, Bethesda, MD20894, USA. Imatinib | C29H31N7O - PubChem. https://pubchem.ncbi.nlm.nih.gov/compound/Imatinib. Accessed July 4, 2022.
101. Kadivar A, Kamalidehghan B, Javar HA, et al. Formulation and In Vitro, In Vivo Evaluation of Effervescent Floating Sustained-Release Imatinib Mesylate Tablet. Sung S-Y, ed. *PLoS One*. 2015;10(6):e0126874. doi:10.1371/journal.pone.0126874
102. Dong Q, Fu X, Du L, et al. Blocking of the Human Ether-à-go-go-Related Gene Channel by Imatinib Mesylate. *Biol Pharm Bull*. 2013;36(2):268-275. doi:10.1248/bpb.b12-00778
103. Peng B, Lloyd P, Schran H. Clinical Pharmacokinetics of Imatinib. *Clin Pharmacokinet*. 2005;44(9):879-894. doi:10.2165/00003088-200544090-00001
104. Peng B, Hayes M, Resta D, et al. Pharmacokinetics and Pharmacodynamics of Imatinib in a Phase I Trial With Chronic Myeloid Leukemia Patients. *J Clin Oncol*. 2004;22(5):935-942. doi:10.1200/JCO.2004.03.050
105. Lee H-A, Hyun S-A, Byun B, Chae J-H, Kim K-S. Electrophysiological mechanisms of vandetanib-induced cardiotoxicity: Comparison of action potentials in rabbit Purkinje fibers and pluripotent stem cell-derived cardiomyocytes. Xu S-Z, ed. *PLoS One*. 2018;13(4):e0195577. doi:10.1371/journal.pone.0195577
106. Deshpande H, Sosa J, Marler. Clinical utility of vandetanib in the treatment of patients with advanced medullary thyroid cancer. *Onco Targets Ther*. 2011;4:209. doi:10.2147/OTT.S17422
107. Lynch TJ, Bell DW, Sordella R, et al. Activating Mutations in the Epidermal Growth Factor Receptor Underlying Responsiveness of Non–Small-Cell Lung Cancer to Gefitinib. *N Engl J Med*. 2004;350(21):2129-2139. doi:10.1056/NEJMoa040938
108. Jie L-J, Li Y-D, Zhang H-Q, et al. Mechanisms of gefitinib-induced QT prolongation. *Eur J Pharmacol*. 2021;910:174441. doi:10.1016/j.ejphar.2021.174441
109. Shah RR, Morganroth J, Shah DR. Cardiovascular Safety of Tyrosine Kinase Inhibitors: With a Special Focus on Cardiac Repolarisation (QT Interval). *Drug Saf*. 2013;36(5):295-316. doi:10.1007/s40264-013-0047-5
110. Kamiya K, Niwa R, Morishima M, Honjo H, Sanguinetti MC. Molecular Determinants of hERG Channel Block by Terfenadine and Cisapride. *J Pharmacol Sci*. 2008;108(3):301-307. doi:10.1254/jphs.08102FP
111. Wang W-T, Chen Y-H, Hsu J-L, et al. Terfenadine induces anti-proliferative and apoptotic activities in human hormone-refractory prostate cancer through histamine receptor-independent Mcl-1 cleavage and Bak up-regulation. *Naunyn Schmiedebergs Arch Pharmacol*. 2014;387(1):33-45. doi:10.1007/s00210-013-0912-x
112. Hadzijusufovic E, Peter B, Gleixner K V., et al. H1-receptor antagonists terfenadine and loratadine inhibit spontaneous growth of neoplastic mast cells. *Exp Hematol*. 2010;38(10):896-907. doi:10.1016/j.exphem.2010.05.008
113. Jangi S-M, Ruiz-Larrea MB, Nicolau-Galmes F, et al. Terfenadine-induced apoptosis in human melanoma cells is mediated through Ca2+ homeostasis modulation and tyrosine kinase activity, independently of H1 histamine receptors. *Carcinogenesis*. 2007;29(3):500-509. doi:10.1093/carcin/bgm292
114. Jangi S-M, Asumendi A, Arlucea J, et al. Apoptosis of Human T-Cell Acute Lymphoblastic Leukemia Cells by Diphenhydramine, an H1 Histamine Receptor Antagonist. *Oncol Res Featur Preclin Clin Cancer Ther*. 2004;14(7):363-372. doi:10.3727/0965040041292369
115. Pratt C, Brown AM, Rampe D, et al. Cardiovascular safety of fexofenadine HCl. *Clin Exp Allergy*. 1999;29(3):212-216. doi:10.1046/j.1365-2222.1999.0290s3212.x
116. Lu HR, Hermans AN, Gallacher DJ. Does terfenadine-induced ventricular tachycardia/fibrillation directly relate to its QT prolongation and Torsades de Pointes? *Br J*

Pharmacol. 2012;166(4):1490-1502. doi:10.1111/j.1476-5381.2012.01880.x
117. Woosley RL. Mechanism of the Cardiotoxic Actions of Terfenadine. *JAMA J Am Med Assoc*. 1993;269(12):1532. doi:10.1001/jama.1993.03500120070028
118. National Center for Biotechnology Information. Terfenadine | C32H41NO2 - PubChem. https://pubchem.ncbi.nlm.nih.gov/compound/Terfenadine. Published 2020. Accessed July 5, 2022.
119. Bookwala M, Gumireddy A, Aitken JA, Wildfong PLD. Single Crystal Structure of Terfenadine Form I. *J Chem Crystallogr*. 2022;52(1):81-88. doi:10.1007/s10870-021-00892-3
120. PubChem Biotechnology National Center. Fexofenadine | C32H39NO4 - PubChem. https://pubchem.ncbi.nlm.nih.gov/compound/Fexofenadine. Accessed July 14, 2022.
121. Vaghela B. Identification and Characterization of an Oxidative Degradation Product of Fexofenadine, Development and Validation of a Stability Indicating RP-UPLC Method for the Estimation of Process Related Impurities and Degradation Products of Fexofenadine in Pharm. *Sci Pharm*. 2012;80(2):295-309. doi:10.3797/scipharm.1111-07
122. Stork D, Timin EN, Berjukow S, et al. State dependent dissociation of HERG channel inhibitors. *Br J Pharmacol*. 2007;151(8):1368-1376. doi:10.1038/sj.bjp.0707356
123. Farid R, Day T, Friesner RA, Pearlstein RA. New insights about HERG blockade obtained from protein modeling, potential energy mapping, and docking studies. *Bioorg Med Chem*. 2006;14(9):3160-3173. doi:10.1016/j.bmc.2005.12.032
124. Rampe DE, Wible B, Brown AM, Dage RC. Effects of terfenadine and its metabolites on a delayed rectifier K+ channel cloned from human heart. *Mol Pharmacol*. 1993;44(6):1240-1245.
125. Roy ML, Dumaine R, Brown AM. HERG, a Primary Human Ventricular Target of the Nonsedating Antihistamine Terfenadine. *Circulation*. 1996;94(4):817-823. doi:10.1161/01.CIR.94.4.817
126. Lang DG, Wang CM, Wenger TL. Terfenadine Alters Action Potentials in Isolated Canine Purkinje Fibers More Than Acrivastine. *J Cardiovasc Pharmacol*. 1993;22(3):438-442. doi:10.1097/00005344-199309000-00014
127. Fritz I, Wagner P, Olsson H. Improved survival in several cancers with use of H1-antihistamines desloratadine and loratadine. *Transl Oncol*. 2021;14(4):101029. doi:10.1016/j.tranon.2021.101029
128. Kong X, Chen L, Jiao L, et al. Astemizole Arrests the Proliferation of Cancer Cells by Disrupting the EZH2-EED Interaction of Polycomb Repressive Complex 2. *J Med Chem*. 2014;57(22):9512-9521. doi:10.1021/jm501230c
129. Crumb WJ. Loratadine blockade of K+ channels in human heart: Comparison with terfenadine under physiological conditions. *J Pharmacol Exp Ther*. 2000;292(1):261-264.
130. Zhou Z, Vorperian VR, Gong Q, Zhang S, January CT. Block of HERG potassium channels by the antihistamine astemizole and its metabolites desmethylastemizole and norastemizole. *J Cardiovasc Electrophysiol*. 1999;10(6):836-843. doi:10.1111/J.1540-8167.1999.TB00264.X
131. Hamoya T, Miyamoto S, Tomono S, et al. Chemopreventive effects of a low-side-effect antibiotic drug, erythromycin, on mouse intestinal tumors. *J Clin Biochem Nutr*. 2017;60(3):199-207. doi:10.3164/jcbn.16-107
132. Pillozzi S, Masselli M, Gasparoli L, et al. Macrolide antibiotics exert antileukemic effects by modulating the autophagic flux through inhibition of hERG1 potassium channels. *Blood Cancer J*. 2016;6(5):e423-e423. doi:10.1038/bcj.2016.32
133. Schoenenberger RA, Haefeli WE, Weiss P, Ritz RF. Association of intravenous erythromycin and potentially fatal ventricular tachycardia with Q-T prolongation (torsades de pointes). *BMJ*. 1990;300(6736):1375-1376. doi:10.1136/bmj.300.6736.1375
134. Nattel S, Ranger S, Talajic M, Lemery R, Roy D. Erythromycin-induced long QT syndrome: Concordance with quinidine and underlying cellular electrophysiologic mechanism. *Am J Med*. 1990;89(2):235-238. doi:10.1016/0002-9343(90)90305-W
135. Katapadi K, Kostandy G, Katapadi M, Hussain KMA, Schifter D, Kostandy G. A Review of Erythromycin-Induced Malignant Tachyarrhythmia— Torsade de Pointes. *Angiology*. 1997;48(9):821-826. doi:10.1177/000331979704800909
136. National Center for Biotechnology Information. Erythromycin | C37H67NO13 - PubChem. National librery of Medicine. https://pubchem.ncbi.nlm.nih.gov/compound/Erythromycin.

Accessed July 6, 2022.
137. Staunton J, Wilkinson B. Biosynthesis of Erythromycin and Related Macrolides. In: *Comprehensive Natural Products Chemistry*. Elsevier; 1999:495-532. doi:10.1016/B978-0-08-091283-7.00020-5
138. Winnicka K, Wroblewska M, Wieczorek P, Sacha P, Tryniszewska E. The Effect of PAMAM Dendrimers on the Antibacterial Activity of Antibiotics with Different Water Solubility. *Molecules*. 2013;18(7):8607-8617. doi:10.3390/molecules18078607
139. Duncan RS, Ridley JM, Dempsey CE, et al. Erythromycin block of the HERG K+ channel: Accessibility to F656 and Y652. *Biochem Biophys Res Commun*. 2006;341(2):500-506. doi:10.1016/j.bbrc.2006.01.008
140. Guo J, Zhan S, Lees-Miller JP, Teng G, Duff HJ. Exaggerated block of hERG (KCNH2) and prolongation of action potential duration by erythromycin at temperatures between 37°C and 42°C. *Hear Rhythm*. 2005;2(8):860-866. doi:10.1016/j.hrthm.2005.04.029
141. Daleau P, Lessard E, Groleau M-F, Turgeon J. Erythromycin Blocks the Rapid Component of the Delayed Rectifier Potassium Current and Lengthens Repolarization of Guinea Pig Ventricular Myocytes. *Circulation*. 1995;91(12):3010-3016. doi:10.1161/01.CIR.91.12.3010
142. Austin K, Mather L, Philpot C, McDonald P. Intersubject and dose-related variability after intravenous administration of erythromycin. *Br J Clin Pharmacol*. 1980;10(3):273-279. doi:10.1111/j.1365-2125.1980.tb01755.x
143. Stanat SJC, Carlton CG, Crumb WJ, Agrawal KC, Clarkson CW. Characterization of the inhibitory effects of erythromycin and clarithromycin on the HERG potassium channel. *Mol Cell Biochem*. 2003;254(1-2):1-7. doi:10.1023/A:1027309703313
144. Volberg WA, Koci BJ, Su W, Lin J, Zhou J. Blockade of Human Cardiac Potassium Channel Human Ether-a-go-go- Related Gene (HERG) by Macrolide Antibiotics. *J Pharmacol Exp Ther*. 2002;302(1):320-327. doi:10.1124/jpet.302.1.320
145. Petroni G, Bagni G, Iorio J, et al. Clarithromycin inhibits autophagy in colorectal cancer by regulating the hERG1 potassium channel interaction with PI3K. *Cell Death Dis*. 2020;11(3):161. doi:10.1038/s41419-020-2349-8
146. Yatsunami J, Tsuruta N, Fukuno Y, Kawashima M, Taniguchi S, Hayashi S ichiro. Inhibitory effects of roxithromycin on tumor angiogenesis, growth and metastasis of mouse B16 melanoma cells. *Clin Exp Metastasis*. 1999;17(2):119-124. doi:10.1023/A:1006591805332
147. Craig Jordan V. The role of tamoxifen in the treatment and prevention of breast cancer. *Curr Probl Cancer*. 1992;16(3):134-176. doi:10.1016/0147-0272(92)90002-6
148. Yu F, Bender W. The mechanism of tamoxifen in breast cancer prevention. *Breast Cancer Res*. 2001;3(S1):A74. doi:10.1186/bcr404
149. Trump DL, Smith DC, Ellis PG, et al. High-Dose Oral Tamoxifen, a Potential Multidrug-Resistance-Reversal Agent: Phase I Trial in Combination With Vinblastine. *JNCI J Natl Cancer Inst*. 1992;84(23):1811-1816. doi:10.1093/jnci/84.23.1811
150. Pollack IF, Darosso RC, Robertson PL, et al. A phase I study of high-dose tamoxifen for the treatment of refractory malignant gliomas of childhood. *Clin Cancer Res*. 1997;3(7):1109-1115. https://aacrjournals-org.proxy.library.uu.nl/clincancerres/article/3/7/1109/7971/A-phase-I-study-of-high-dose-tamoxifen-for-the. Accessed July 7, 2022.
151. Hoskins JM, Carey LA, McLeod HL. CYP2D6 and tamoxifen: DNA matters in breast cancer. *Nat Rev Cancer*. 2009;9(8):576-586. doi:10.1038/nrc2683
152. Holmes FA, Liticker JD. Pharmacogenomics of Tamoxifen in a Nutshell—And Who Broke the Nutcracker? *J Oncol Pract*. 2005;1(4):155-159. doi:10.1200/jop.2005.1.4.155
153. Jin Y, Desta Z, Stearns V, et al. CYP2D6 Genotype, Antidepressant Use, and Tamoxifen Metabolism During Adjuvant Breast Cancer Treatment. *JNCI J Natl Cancer Inst*. 2005;97(1):30-39. doi:10.1093/jnci/dji005
154. PubChem. *Tamoxifen | C26H29NO - PubChem*. Vol 13.; 2022. https://pubchem.ncbi.nlm.nih.gov/compound/Tamoxifen. Accessed July 8, 2022.
155. De Filippis B, Ammazzalorso A, Fantacuzzi M, Giampietro L, Maccallini C, Amoroso R. Anticancer Activity of Stilbene-Based Derivatives. *ChemMedChem*. 2017;12(8):558-570. doi:10.1002/cmdc.201700045
156. Endoxifen | C25H27NO2 - PubChem. https://pubchem.ncbi.nlm.nih.gov/compound/Endoxifen.

Accessed July 8, 2022.
157. Ahmad A, Sheikh S, Shah T, et al. Endoxifen, a New Treatment Option for Mania: A Double-Blind, Active-Controlled Trial Demonstrates the Antimanic Efficacy of Endoxifen. *Clin Transl Sci*. 2016;9(5):252-259. doi:10.1111/cts.12407
158. Thomas D, Gut B, Karsai S, et al. Inhibition of cloned HERG potassium channels by the antiestrogen tamoxifen. *Naunyn Schmiedebergs Arch Pharmacol*. 2003;368(1):41-48. doi:10.1007/s00210-003-0766-8
159. Chae YJ, Lee KJ, Lee HJ, et al. Endoxifen, the active metabolite of tamoxifen, inhibits cloned hERG potassium channels. *Eur J Pharmacol*. 2015;752:1-7. doi:10.1016/j.ejphar.2015.01.048
160. Liu XKE, Katchman A, Ebert SN, Woosley RL. The antiestrogen tamoxifen blocks the delayed rectifier potassium current, IKP in rabbit ventricular myocytes. *J Pharmacol Exp Ther*. 1998;287(3):877-883.
161. DANIEL CP, GASKELL SJ, BISHOP H, NICHOLSON RI. DETERMINATION OF TAMOXIFEN AND AN HYDROXYLATED METABOLITE IN PLASMA FROM PATIENTS WITH ADVANCED BREAST CANCER USING GAS CHROMATOGRAPHY–MASS SPECTROMETRY. *J Endocrinol*. 1979;83(3):401-408. doi:10.1677/joe.0.0830401
162. Murphy C, Fotsis T, Pantzar P, Adlercreut H, Martin F. Analysis of tamoxifen and its metabolites in human plasma by gas chromatography-mass spectrometry (GC-MS) using selected ion monitoring (SIM). *J Steroid Biochem*. 1987;26(5):547-555. doi:10.1016/0022-4731(87)90006-9
163. Berman E, McBride M, Lin S, Menedez-Botet C, Tong W. Phase I trial of high-dose tamoxifen as a modulator of drug resistance in combination with daunorubicin in patients with relapsed or refractory acute leukemia. *Leukemia*. 1995;9(10):1631-1637. https://pubmed.ncbi.nlm.nih.gov/7564501/. Accessed July 8, 2022.
164. Bergan RC, Reed E, Myers CE, et al. A Phase II study of high-dose tamoxifen in patients with hormone- refractory prostate cancer. *Clin Cancer Res*. 1999;5(9):2366-2373. https://pubmed.ncbi.nlm.nih.gov/10499606/. Accessed July 8, 2022.
165. Albini A, Pennesi G, Donatelli F, Cammarota R, De Flora S, Noonan DM. Cardiotoxicity of Anticancer Drugs: The Need for Cardio-Oncology and Cardio-Oncological Prevention. *JNCI J Natl Cancer Inst*. 2010;102(1):14-25. doi:10.1093/jnci/djp440